JOURNAL OF GEOPHYSICAL RESEARCH, VOL. 86, NO. B4, PAGES 2721-2735, APRIL 10, 1981

Sm-Nd, Rb-Sr, and $^{18}O/^{16}O$ Isotopic Systematics in an Oceanic Crustal Section: Evidence From the Samail Ophiolite

MALCOLM T. MCCULLOCH,[1] ROBERT T. GREGORY, G. J. WASSERBURG,[1] AND HUGH P. TAYLOR, JR.

Division of Geological and Planetary Sciences, California Institute of Technology, Pasadena, California 91125

The Sm-Nd, Rb-Sr, and $^{18}O/^{16}O$ isotopic systems have been used to distinguish between the effects of seafloor hydrothermal alteration and primary magmatic isotopic variations. The Sm-Nd isotopic system is essentially unaffected by seawater alteration, while the Rb-Sr and $^{18}O/^{16}O$ systems are sensitive to hydrothermal interactions with seawater. Sm-Nd mineral isochrons from the cumulate gabbros of the Samail ophiolite have an initial $^{143}Nd/^{144}Nd$ ratio of $\epsilon_{Nd} = 7.8 \pm 0.3$, which clearly substantiates the oceanic affinity of this complex. The initial $^{143}Nd/^{144}Nd$ ratios for the harzburgite, plagiogranite, sheeted diabase dikes, and basalt units have a limited range in ϵ_{Nd} of from 7.5 to 8.6, indicating that all the lithologies have distinctive oceanic affinities, although there is also some evidence for small isotopic heterogeneities in the magma reservoirs. The Sm-Nd mineral isochrons give crystallization ages of 128 ± 20 m.y. and 150 ± 40 m.y. from Ibra and 100 ± 20 m.y. from Wadi Fizh, which is approximately 300 km NW of Ibra. These crystallization ages are interpreted as the time of formation of the oceanic crust. The $^{87}Sr/^{86}Sr$ initial ratios on the same rocks have an extremely large range of from 0.7030 to 0.7065 and the $\delta^{18}O$ values vary from 2.6 to 12.7. These large variations clearly demonstrate hydrothermal interaction of oceanic crust with seawater.

INTRODUCTION

The purpose of this study is to compare the neodymium, strontium, and oxygen isotopic characteristics of the Samail ophilite, Oman. These rocks are of significance, as it is now generally recognized that ophiolites represent transported slabs of oceanic crust and upper mantle emplaced upon continental margins. The Samail ophiolite provides a unique opportunity to study in detail a well-exposed and preserved section of oceanic crust. The Samail, unlike most other 'dismembered' ophiolites, is remarkably intact with a thickness comparing favorably to geophysical estimates of typical oceanic crustal sections [*Coleman*, 1977; *Christensen and Salisbury*, 1975]. Because of its enormous size (exposed over most of the 700-km-long Oman Mountains) it has been possible to contrast isotopic variations within a single tectonic unit over large distances perpendicular to the presumed paleospreading direction.

The Nd, Sr, and O isotopic characteristics were determined on identical samples from the harzburgite, gabbro, plagiogranite, sheeted dikes, and basalt units. The $^{18}O/^{16}O$ and Rb-Sr isotopic systems are sensitive to hydrothermal exchange with seawater [*Taylor*, 1968; *Muehlenbachs and Clayton*, 1972; *Peterman et al.*, 1971; *Spooner et al.*, 1977]. Using $\delta^{18}O$ variations as a criteria, samples were selected for Nd-Sr analyses which exhibited either slight effects of subsolidus hydrothermal exchange or pervasive amounts of high or low temperature exchange. By analyzing both fresh and altered samples, as identified by the oxygen and strontium data, the effect of seawater alteration upon the Sm-Nd system could be evaluated.

Sm-Nd isotopic studies of mafic rocks by *Lugmair et al.* [1976], *Nakamura et al.* [1976], *DePaolo and Wasserburg* [1979], and *Hamilton et al.* [1979] have shown that crystallization ages can, in general, be obtained from coexisting plagioclase and pyroxene. In addition, Nd isotopic studies of young midocean ridge basalts (MORB) by *O'Nions et al.* [1977] and *DePaolo and Wasserburg* [1977] have shown that the Nd isotopic composition is apparently unaffected by hydrothermal interactions. For these reasons the feasibility of obtaining Sm-Nd crystallization ages from the gabbro members of the Samail ophiolite was investigated. The determination of Sm-Nd crystallization ages from ophiolites has many potential applications, as most ophiolitic material is unsuitable for isotopic dating by other techniques. An exception is the dating by U-Pb of zircons sometimes found in plagiogranites and in the more differentiated hornblende gabbros [*Tilton et al.*, 1981].

A preliminary Nd isotopic study by *Richard et al.* [1978] of single whole rock gabbro samples from the Troodos, Samail, and several other ophiolite complexes has shown that the measured $^{143}Nd/^{144}Nd$ ratios are similar to those found in young ocean floor basalts [*DePaolo and Wasserburg*, 1976*a*, *b*; *O'Nions et al.*, 1977]. This study presents a more comprehensive analysis of the results of *McCulloch et al.* [1980].

Geology and Sampling

The Samail ophiolite forms a major part of the 700 km long arcuate Oman Mountains which are on the eastern edge of the Arabian Peninsula (Figure 1). The samples analyzed in this study mainly come from the Ibra ophiolite section southeastern Oman (see Figure 1). A detailed geologic map of the Ibra section in southeastern Oman is given by *Bailey* [1981]. In addition to the samples from Ibra, two cumulate gabbro samples (OM251 and OM28) from the Rustaq and Wadi Fizh localities (Figure 1) were also analyzed to check for regional isotopic and age variations within similar lithologies of the ophiolite on a scale of several hundred kilometers.

A minimum age for the emplacement of the ophiolite is provided by Maestrichtian-Tertiary shallow water limestones which unconformably overlie parts of the ophiolite. A maximum age is given by K-Ar ages of ~90 m.y. (Turonian) [*Lanphere*, 1981] from metamorphic biotites in amphibolites from the detachment aureole at base of the Samail thrust sheet. Until now (see also *Tilton et al.* [1981]) evidence for the age of production of the oceanic crust is sparse, although *Glennie et al.* [1974] estimated a minimum age limit based on middle to

[1] Lunatic Asylum of the Charles Arms Laboratory, California Institute of Technology, Pasadena, California 91125.

Paper number 80B0930.
0148-0227/81/080B-0930$01.00

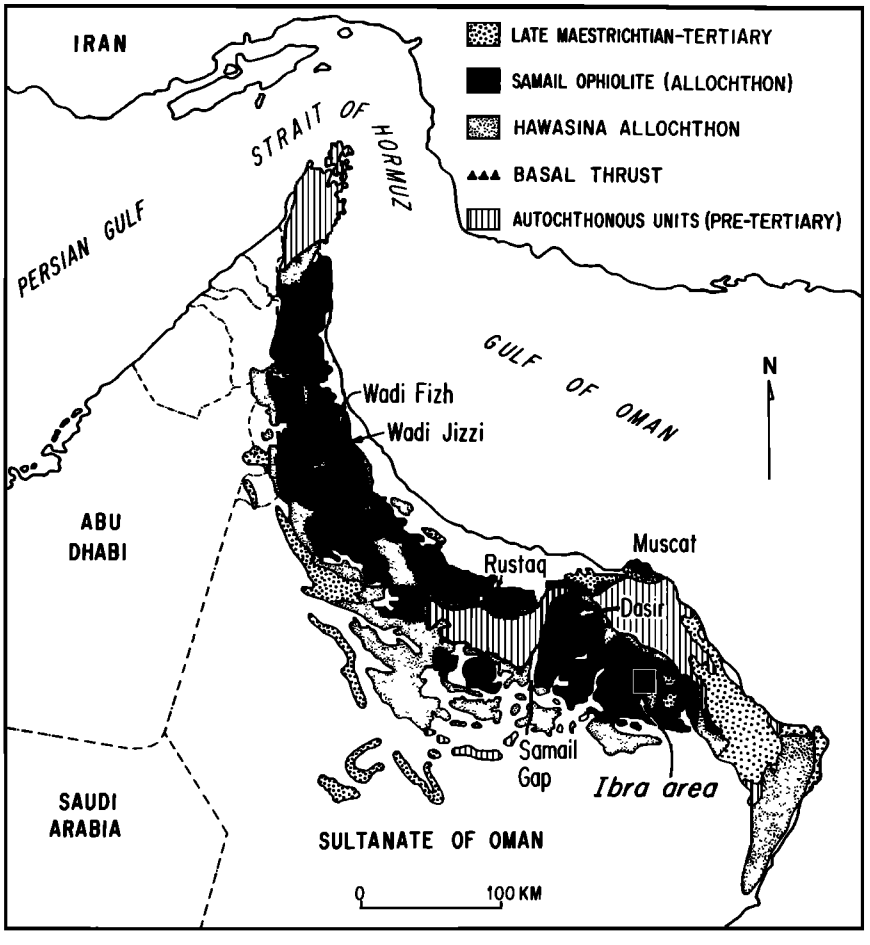

Fig. 1. Simplified geologic map of the Samail ophiolite, Oman [after *Glennie et al.*, 1974], showing sample localities. The Samail ophiolite (solid) is an allochtonous body which is in thrust contact with the underlying rocks.

late Cretaceous (Cenomanian) sediments which overlie the pillow lavas in northern Oman.

Sample Descriptions

The stratigraphic locality of the Ibra samples is shown in Figure 11.

Basalt G54 (Ibra). Microphyric basalt with acicular laths of plagioclase (An_{25}). Groundmass is altered to palagonite, zeolites (?), saponite (?), and calcite. The calcite is present as 1–2 cm amygdules and also as smaller blebs dispersed throughout the rock. A whole rock sample which was free of large amygdules and calcite from an amygdule were analyzed. The mineralogy and oxygen isotope data (whole rock $\delta^{18}O$ = 12.7) are consistent with low temperature alteration (100°–200°C).

Diabase dike G10 (Ibra). Ophitic texture with turbid albitized plagioclase (An_{20}). Alteration products include epidote, chlorite, antinolite-tremolite pseudomorphs after pyroxene, quartz, carbonate, and leucoxene. The mineralogy indicates alteration in the greenschist facies.

Diabase dike K1 (Ibra). Ophitic texture with turbid plagioclase (An_{25}), clinopyroxene, and opaques. Alteration products include chlorite, uralite, and quartz and suggest alteration at greenschist facies.

Plagiogranite G224-3 (Ibra). Granophyric texture with zoned plagioclase (core An_{30}, rim An_{25}), hornblende, quartz, magnetite, and trace amounts of apatite. Hornblende is partially altered to uralite. The plagiogranite was collected from a nonchilled dike which cross-cuts uralite gabbro, G224-2, approximately 500 m below the gabbro-diabase contact.

Uralite gabbro G224-2 (Ibra). Poikilitic hornblende enclosing zoned plagioclase (core An_{40}, rim An_{20}) and opaques. Alteration products include fibrous amphibole pseudomorphs after hornblende, chlorite, and rare prehnite. The mineralogy and oxygen isotope data (whole rock $\delta^{18}O$ = 3.7, plagioclase $\delta^{18}O$ = 4.5, and uralite $\delta^{18}O$ = 2.6) suggest relatively high temperatures of alteration (>400°C).

Gabbro K9 (Ibra). Adcumulate with igneous lamination; 72% plagioclase (An_{75}), 20% clinopyroxene, 7% olivine, and 1% hornblende. The brown hornblende is a minor alteration product of the clinopyroxene. The mineralogy and oxygen isotope data (whole rock $\delta^{18}O$ = 5.8, plagioclase $\delta^{18}O$ = 6.0, and clinopyroxene $\delta^{18}O$ = 5.3) indicate that this is one of the least altered samples.

Gabbro OM251 (Wadi Fizh, northern Oman). Late cumulate pyroxene poikilitically enclosing plagioclase; 77% plagioclase (An_{80}), 20% clinopyroxene, and 3% olivine. The olivine has been partially serpentinized. Although the olivine is serpentinized, the oxygen data (plagioclase $\delta^{18}O$ = 6.4 and clinopyroxene $\delta^{18}O$ = 5.8) indicate that the plagioclase and clinopyroxene have exchanged only slightly with an ^{18}O shifted seawater-derived hydrothermal fluid.

Gabbro OM28 (Rustaq). Adcumulate with igneous lamination; 72% plagioclase (An_{75}), 15% clinopyroxene, 10% am-

TABLE 1. Nd, Sr, and O Isotopic Data From the Samail Ophiolite

Samples	$\frac{^{87}Rb}{^{86}Sr}$	$\frac{^{147}Sm}{^{144}Nd}$	$\frac{^{87}Sr}{^{86}Sr}$	$\frac{^{143}Nd}{^{144}Nd}$	ϵ_{Sr}*	ϵ_{Nd}*	$\delta^{18}O$
Basalt							
G54 WR	0.104	0.192	0.70491 ± 4	0.512219 ± 19	5.3 ± 0.6	7.5 ± 0.4	12.7
G54 Calcite	0.004	0.209	0.70650 ± 15	0.512265 ± 29	30.5 ± 2.1	8.1 ± 0.6	
Sheeted Dikes							
G10	0.029	0.209	0.70535 ± 4	0.512250 ± 25	13.5 ± 0.6	7.8 ± 0.5	8.5
K1	0.008	0.194	0.70519 ± 4	0.512275 ± 20	11.7 ± 0.6	8.6 ± 0.4	6.8
Plagiogranite							
G224-3	0.035	0.187	0.70362 ± 4	0.512249 ± 18	−11.3 ± 0.6	8.2 ± 0.3	5.2
Gabbros							
G224-2 WR	0.010	0.201	0.70370 ± 3	0.512251 ± 19	−9.5 ± 0.4	8.0 ± 0.4	3.7
G224-2 PLAG	0.008	0.151	0.70352 ± 4	0.512196 ± 18	−12.0 ± 0.6	7.8 ± 0.3	4.5
G224-2 URAL	0.014	0.241	0.70426 ± 3	0.512285 ± 19	−1.6 ± 0.4	8.0 ± 0.4	2.6
K9 WR	0.0008	0.271	0.70304 ± 5	0.512310 ± 18	−18.6 ± 0.7	8.0 ± 0.3	5.7
K9 PLAG	0.0005	0.129	0.70296 ± 2	0.512180 ± 25	−19.7 ± 0.3	7.8 ± 0.5	6.0
				0.512181 ± 19†		7.8 ± 0.4	
K9 CPX	0.0008	0.322	0.70313 ± 3	0.512341 ± 15	−17.3 ± 0.4	7.7 ± 0.3	5.3
		0.316		0.512332 ± 22†		7.7 ± 0.4	
OM251 PLAG	0.0010	0.159	0.70311 ± 5	0.512203 ± 22	−18.0 ± 0.7	7.6 ± 0.4	6.4
OM251 CPX	0.0018	0.377	0.70315 ± 5	0.512346 ± 25†	−17.5 ± 0.7	7.6 ± 0.5	5.8
OM28 WR	0.0014	0.264	0.70383 ± 5	0.512274 ± 22†	−7.8 ± 0.7	7.7 ± 0.4	5.2
Harzburgite							
K22	0.150	0.216	0.70313 ± 9	0.512278 ± 23	−21.2 ± 1.1	8.3 ± 0.4	

*The ϵ_{Sr} and ϵ_{Nd} values calculated for a crystallization age of 130 m.y. except for OM251 and OM28 for which an age of 100 m.y. was used.
†The $^{143}Nd/^{144}Nd$ determined from spiked sample.

phibole, and 2% serpentine, and/or talc alteration pseudomorphing olivine. In contrast to the other cumulate gabbros, the oxygen isotope data from this sample (plagioclase $\delta^{18}O$ = 4.7 and whole rock $\delta^{18}O$ = 5.2) indicate significant exchange of plagioclase and pyroxene with a seawater-derived fluid.

Harzburgite K22 (Ibra). Porphyroclastic texture with tectonite fabric; 25% orthopyroxene, 45% olivine, 30% serpentine, and trace amounts of spinel. Serpentine is pseudomorphing olivine.

Experimental Procedures

Samples were prepared by removing exterior surfaces with a rock splitter and crushing interior chunks. Only mechanical means were used for mineral separation and involved a combination of handpicking and magnetic separation. These procedures produced high purity (~100%) plagioclase separates and pyroxene separates of greater than 95% purity. The small amount of impurity in the pyroxene separate generally consisted of olivine which is unimportant as it contains extremely low trace element concentrations.

Oxygen was extracted and analyzed from approximately 20 mg of sample using the procedures outlined by *Taylor and Epstein* [1962]. For Nd and Sr approximately 200 mg of sample was dissolved using HF and $HClO_4$. After complete dissolution an aliquot consisting of about 10% of the solution was spiked and concentrations of K, Rb, Sr, Sm, and Nd were determined. From approximately 100 mg of the remaining unspiked solution, Nd and Sr were separated using ion exchange chemistry. For several samples (see Table 1) both Sm and Nd concentrations and $^{143}Nd/^{144}Nd$ ratios were obtained from the same spiked sample. For the plagioclase separate from the gabbro K9, the $^{143}Nd/^{144}Nd$ ratio was obtained from both spiked and unspiked samples and was the same within experimental error. The Sr isotopic composition was measured using a single oxidized tantalum filament, and typically ~150 ratios were collected. The Nd isotopic composition was determined by measuring NdO^+ on a single rhenium filament and normalized to $^{150}Nd/^{142}Nd$ = 0.2096. The 2σ (mean) errors quoted for the $^{143}Nd/^{144}Nd$ ratio were generally obtained from about 250 ratios. For the above procedures the blanks were Rb = 0.01 ng, Sr = 0.1 ng, Sm = 0.006 ng, and Nd = 0.02 ng and are negligible for the data presented here.

For the harzburgite the lower Sr and Nd concentrations required the use of a slightly modified procedure to enable the precise determination of the isotopic compositions. Approximately 400 mg of the harzburgite was dissolved and split into three equal portions after removing a 10% aliquot for concentrations. The three portions were passed separately through a cation column, and Sr and rare earths were separated. The rare earth fractions were combined and loaded on the lactic acid column, and Nd was separated. Using this procedure, a total of 10 ng of Nd was obtained from the harzburgite K22, with a Nd blank of ~0.06 ng. This blank is less than 0.6% of the total Nd and is therefore still insignificant. For 10 ng of Nd the precision of the $^{143}Nd/^{144}Nd$ ratio is still better than 5 parts in 10^5.

Data Representation

The oxygen data are given in the conventional δ notation of

$$\delta^{18}O = [(^{18}O/^{16}O)_{sample}/(^{18}O/^{16}O)_{standard} - 1]\ 10^3$$

Samples are corrected to the SMOW scale using California Institute of Technology rose quartz $\delta^{18}O$ = 8.45. Following *DePaolo and Wasserburg* [1976a], an analogous notation is used for Nd and Sr, with the reference reservoir evolving with time where

$$\epsilon_{Nd} = [(^{143}Nd/^{144}Nd)_{INIT}{}^{T}/(^{143}Nd/^{144}Nd)_{CHUR}{}^{T} - 1]\ 10^4$$

and

$$\epsilon_{Sr} = [(^{87}Sr/^{86}Sr)_{INIT}{}^{T}/(^{87}Sr/^{86}Sr)_{UR}{}^{T} - 1]\ 10^4$$

The $(^{143}Nd/^{144}Nd)_{INIT}{}^{T}$ and $(^{87}Sr/^{86}Sr)_{INIT}{}^{T}$ are the measured ratios corrected for decay since the time of crystallization T.

The $(^{143}Nd/^{144}Nd)_{CHUR}{}^{T}$ and $(^{87}Sr/^{86}Sr)_{UR}{}^{T}$ ratios are those in the standard reservoirs [*DePaolo and Wasserburg, 1976a, b*] at the time T.

Results

Oxygen Isotopic Characteristics

The oxygen isotopic systematics of the Samail ophiolite are discussed in detail by *Gregory and Taylor* [1981]. The three general categories of samples are (1) lower cumulate gabbros which exhibit close to 'normal' ^{18}O characteristics (K9, OM251), (2) rocks below the diabase-gabbro contact which exhibit ^{18}O depletions (G224-2, G224-3, OM28), and (3) rocks above the diabase-gabbro contact which exhibit ^{18}O enrichments, relative to a MORB reservoir of $\delta^{18}O = 5.7$ [*Muehlenbachs and Clayton, 1976*]. The dichotomy between $\delta^{18}O$ values of the rocks above or below the diabase-gabbro contact is a result of differing alteration environments which depend upon temperature, water/rock ratio, and the history of the exchanging fluid.

In order to understand the ^{18}O variation due to temperature effects, let us consider the ^{18}O fractionation between rock and fluid defined as

$$\Delta^{18}O_{rock} = \Delta \equiv \delta^{18}O_{rock} - \delta^{18}O_{water} \quad (1)$$

which is a function of temperature given by *Taylor* [1974]:

$$\Delta(T) = \frac{A}{T^2} + B \quad (2)$$

where A, B are constants.

In the basalt-seawater system, temperatures of alteration in the vicinity of 250°C to 300°C produce no ^{18}O shifts in the rocks as a result of hydrothermal exchange (i.e., $\Delta \approx 5.7$). The gabbros which are altered at temperatures greater than 400°C are depleted in $\delta^{18}O$ (i.e., $\Delta < 5.7$). The subsolidus alteration event is characterized by isotopic disequilibrium between coexisting plagioclases and clinopyroxenes and water/rock ratios <1.0 [*Gregory and Taylor, 1981*]. The Samail gabbro-water interactions are analogous to those observed in continental layered complexes such as the Skaergaard intrusion which have suffered meteoric hydrothermal exchange [*Taylor and Forester, 1979*]. The major difference between the continental and marine environments is the contrast between the initial compositions of the hydrothermal fluids: meteoric water with an initial $\delta^{18}O \sim -15‰$ (e.g., the Skaergaard [*Taylor and Forester, 1979*]), and seawater with $\delta^{18}O \sim 0‰$. The contrast between fluid and rock in the subaerial environments is large, ~20‰, so that the hydrothermal exchange with meteoric water produces almost exclusively ^{18}O depletions in the intrusion and its surrounding country rock over a wide range of temperatures [*Taylor, 1974; Taylor and Forester, 1979*]. In the marine case, because seawater is isotopically closer to the initial rock composition, the effects of high temperature alteration in the gabbros are less pronounced with a maximum $\delta^{18}O$ depletion of approximately 3‰, while in subaerial environments hydrothermally altered gabbros often display $\delta^{18}O$ depletions of as much as 5–10‰ [*Taylor and Forester, 1979*]. Because of the spreading environment of the seafloor the diabases and pillow lavas overlying gabbroic magma chambers 'see' a time-temperature superposition of alteration regimes that has no other analog in the subaerial examples described to date [*Gregory and Taylor, 1981*].

In order to illustrate these points, considering only the effects of temperature, the diabase dikes altered under greenschist to lower amphibolite facies are expected to be depleted in ^{18}O relative to their primary values if pristine seawater with a $\delta^{18}O \approx -0.5$ is the hydrothermal fluid. However, diabases G10 and K1 with $\delta^{18}O = 8.5, 6.8$, respectively, are to the contrary enriched in ^{18}O. This contradiction requires that these diabases have exchanged with a seawater-derived hydrothermal fluid that has become ^{18}O enriched relative to its initial value. The fluids which have exchanged with the underlying solidified cumulate gabbro are likely candidates as the gabbro section is a region of high-temperature (>400°C) alteration and low water/rock ratio (<1); this is ideal for producing a fluid phase with ^{18}O enrichments. Fluids discharging from the gabbros into the diabases have a calculated ^{18}O enrichment relative to an initial $\delta^{18}O \simeq -0.5$ from ~+2 to ~+9‰ [*Gregory and Taylor, 1981*]. Since seawater is only ~6‰ lighter than the rock, water exhibiting enrichments of this magnitude reacts with the diabases at lower temperature resulting in greenschist facies rocks ($2 \lesssim \Delta(T) \lesssim 6$) with a $\delta^{18}O > 6$. This suggests that the oxygen isotopes of the diabases are recording a final exchange event as the following discussion will illustrate.

The inferred funnel-shaped geometry of the oceanic crustal magma chamber [*Hopson et al., 1981; Pallister and Hopson, 1980*] requires that fluids which exchange with large amounts of solidified gabbro discharge at the distal edge of the chamber away from the ridge axis [*Gregory and Taylor, 1981*]. Since thin sheets of magma (inferred from the crystallization of the most fractionated magma at the diabase-gabbro contact [*Pallister and Hopson, 1980*]; see Figure 11) act as impermeable barriers to fluid circulation [*Taylor and Forester, 1979; Norton and Taylor, 1979*], two hydrothermal systems exist during the early history of newly created oceanic crust: one affecting the roof rocks of the gabbroic magma chamber near the ridge axis and the second affecting the gabbros which have crystallized under the wings of the chamber [*Gregory and Taylor, 1979*]. Waters discharging from the second system react with the diabases which have been already altered by the upper system as they spread away from the ridge axis, and thus the diabases are affected by both systems. These geometrical constraints become important when evaluating the combined Sr and O effects discussed below.

Trace Element Abundances

The K, Rb, Sr, Sm, and Nd abundances are listed in Table 2. The most obvious feature is the contrast in K, Rb, Sm, and Nd concentrations between the layered gabbros (K9, OM28, and OM251) which are a factor of 10 to 100 times lower than those in the upper sequence (plagiogranite, uralite gabbro, sheeted dikes, and basalts). This feature reflects the mineralogy (clinopyroxene, plagioclase, and olivine) and the cumulate origin of the layered gabbros. Since the K, Rb, Sm, and Nd mineral/liquid partition coefficients of the cumulus phases are all less than unity, the gabbro cumulates have much lower concentrations than the melts from which they crystallized. The resulting melt which is enriched in these elements is presumably represented by the overlying more fractionated rocks such as the diabases and pillow basalts. It is therefore unlikely that any particular ophiolite member represents the primitive melt composition. In contrast, the Sr concentration is relatively uniform throughout the layered gabbros and the upper sequence. This is probably due to the high concentration of Sr in plagioclase of the layered gabbro which compensates for

TABLE 2. Trace Element Abundances From the Samail Ophiolite

Samples	K	Rb	Sr	Sm	Nd	Sr/Rb	K/Rb	Sm/Nd
Basalt								
G54 WR	4470	7.16	198	5.03	15.9	28	624	0.316
G54 Calcite	76	0.009	6.12	0.043	0.126	680	8440	0.341
Sheeted Dikes								
G10	3950	1.63	162	3.85	11.2	99	2420	0.344
K1	2290	1.04	388	4.16	13.0	370	2201	0.320
Plagiogranite								
G224-3	2200	2.31	192	5.36	17.3	83	952	0.310
Gabbros								
G224-2 WR	1320	0.674	196	2.78	8.36	290	1960	0.333
G224-2 PLAG	1800	0.950	330	0.563	2.25	350	1890	0.250
G224-2 URAL	740	0.280	58.7	3.79	9.51	210	2640	0.399
K9 WR	117	0.052	188	0.441	0.986	3610	2250	0.447
K9 PLAG	161	0.050	311	0.085	0.399	6220	3220	0.213
K9 CPX	29	0.023	24.8	1.401	2.630	1080	1260	0.533
OM251 PLAG	77	0.055	156	0.021	0.081	2840	1400	0.259
OM251 CPX	20	0.034	54.2	0.256	0.411	1590	588	0.623
OM28 WR	126	0.066	132	0.168	0.385	2000	1910	0.436
Harzburgite								
K22	6	0.023	0.43	0.013	0.035	19	261	0.371
Average MOR* tholeiite	1300	1	130	2.7	8	130	1300	0.34

Parts per million.
*Data from *Engel et al.* [1965], *Tatsumoto et al.* [1965], *Kay et al.* [1970], and *Schilling* [1971].

the lower concentrations in the other cumulate minerals, olivine and clinopyroxene, leaving Sr in the melt approximately constant.

Significant variations in concentrations also exist within the same lithologic units. The gabbro K9 has approximately a factor of 4 higher concentration of Sm and Nd and a factor of approximately 2 higher K and Sr concentrations than the gabbro OM251 (see Table 2). Similar variations have also been observed in the gabbros from the Troodos ophiolite [*Kay and Senechal,* 1976]. The variations in trace element concentration probably reflect the complex crystal fractionation and replenishment history of the magma chamber. In the Samail ophiolite, evidence for multiple cycles of primitive magma replenishment has been extensively documented within the gabbro complex by *Pallister and Hopson* [1981]. This is a common feature of ophiolite complexes [*Moores,* 1969; *Jackson et al.,* 1975] as well as of layered gabbro intrusions emplaced in continental environments, such as the Muskox, Bushveld, and Great Dike intrusions [*Jackson,* 1970, 1971; *Irvine,* 1970].

Trace element concentration variations of the alkali elements may be due to the effects of seawater alteration. Within the upper sequence the K concentration decreases systematically from top to bottom. Rb shows a similar trend to K with the exception of the plagiogranite (G224-3). However, the Sr, Sm, and Nd concentrations do not show any similar systematic trends. This suggests that the higher K and Rb concentrations are due to seawater alteration and are not primary. This is consistent with other studies [*Hart,* 1970; *Chapman and Spooner,* 1977] and observations of K-rich alteration minerals in oceanic basalts [*Seyfried et al.,* 1978]. The end-member (~350°C) water issuing from submarine hot springs [*Corliss et al.,* 1979; *Edmond et al.,* 1979] is enriched in K and Rb relative to normal seawater. These data suggest that K and Rb may have been leached from the deeper levels of the ophiolite complex and preferentially fixed in the upper part of the sequence. Despite the effects of alteration, the K and, to a lesser extent, Rb concentrations of the basaltic rocks are still consistent with an oceanic affinity. The K/Rb ratios of 620 and 2420 and Sr/Rb ratios of 27 to 373 of the diabase dikes and basalt in the Samail ophiolite are roughly comparable to the average midocean ridge (MOR) tholeiite ratios of $K/Rb \simeq 1300$ and $Sr/Rb \simeq 130$ [*Engel et al.,* 1965; *Tatsumoto et al.,* 1965]. The Sm/Nd ratios are within the range of typical MOR tholeiites [*Kay et al.,* 1970; *Schilling,* 1971], while the Sm and Nd concentrations in the Ibra section of the Samail ophiolite are somewhat higher.

The harzburgite, K22, has distinctly lower trace element concentrations than the rest of the ophiolite membes (Table 2). Extremely low concentrations of incompatible elements are common in metamorphic peridotites from other ophiolites and are interpreted as evidence that the harzburgite tectonite is a residual fraction of upper mantle left after partial melting. REE data can also be used [*Montigny et al.,* 1973; *Allegre et al.,* 1973; *Pallister and Knight,* 1981] to test the hypothesis that the harzburgite is a residue cogenetic with the overlying cumulate gabbros and basaltic suites. This type of calculation requires assumptions concerning amount of partial melting, distribution coefficients, and composition of source material, all of which are uncertain. A more definitive constraint is provided by the Nd isotopic data, presented in the following section.

Crystallization Age and Initial $^{143}Nd/^{144}Nd$

Although current models for the formation of ophiolites at spreading centers indicate that within a single section all the igneous rocks, with perhaps the exception of the basal peridotites, should be of approximately the same age, there may still be significant variations in initial $^{143}Nd/^{144}Nd$ ratios due to mantle source heterogeneities. For this reason, analyses of only whole rock samples from different parts of an ophiolite may have variable initial $^{143}Nd/^{144}Nd$ ratios and may not define an isochron. In addition, the range in Sm/Nd ratios of total rocks may be inadequate to define an age for such young samples. Therefore crystallization ages and intial ratios were determined using coexisting minerals separated from gabbros.

We obtained Sm-Nd mineral isochrons from three gabbros

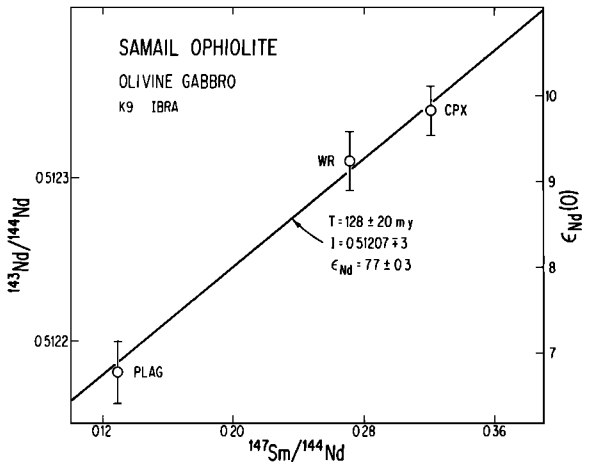

Fig. 2. Sm-Nd evolution diagram for the cumulate gabbro K9, from the Ibra section, Oman. The uncertainty in the age determination is largely controlled by the difference between the $^{147}Sm/^{144}Nd$ ratios of the coexisting clinopyroxene and plagioclase. The $\epsilon_{Nd}(0)$ values are the deviations in parts in 10^4 of the measured $^{143}Nd/^{144}Nd$ ratio from the value in CHUR today (0.511836).

(K9, G224-2, OM251) using plagioclase, clinopyroxene, and uralite mineral separates. The gabbro K9 from the Ibra section contains plagioclase, clinopyroxene, and olivine and is extremely fresh, with only a minor amount of alteration. It can be seen in Table 1 and Figure 2 that the $^{143}Nd/^{144}Nd$ ratio is enriched in the clinopyroxene from K9 by 2 parts in 10^4 relative to the plagioclase. The clinopyroxene also has a higher $^{147}Sm/^{144}Nd$ ratio of 0.320 compared to 0.129 for the plagioclase. Assuming that these minerals and the whole rocks have remained closed systems since crystallizing from an isotopically homogeneous melt, these data indicate a crystallization age of 128 ± 20 m.y. with an initial $^{143}Nd/^{144}Nd$ ratio of ϵ_{Nd} = 7.7 ± 0.3. Since the age and initial ratio for this gabbro are only defined by two independent points, the interpretation of this 'two-point isochron' as the time of crystallization is not unique. To eliminate the possibility of two component mixing producing this array, three or more distinct mineral phases would have to be analyzed. This is not possible in this sample, as no other REE bearing mineral phase is present (olivine contains negligible REE).

We analyzed a second gabbro from the upper part of the same gabbro unit as K9. This gabbro (G224-2) contains uralite as a late-stage replacement of pyroxene and primary hornblende. The low $\delta^{18}O$ values for both plagioclase and uralite indicate that this sample has exchanged with seawater at high temperatures (>400°C). The Sm-Nd data from G224-2 are shown in Table 1 and Figure 3. The uralite has the highest $^{147}Sm/^{144}Nd$ and $^{143}Nd/^{144}Nd$ ratios and together with the plagioclase gives an age of 150 ± 40 m.y. and an initial $^{143}Nd/^{144}Nd$ ratio of ϵ_{Nd} = 7.8 ± 0.4. The larger uncertainty in the age compared to K9 is due to the smaller difference between the $^{147}Sm/^{144}Nd$ ratios in the plagioclase and uralite mineral separates. However, within analytical uncertainty, both samples have the same age and initial $^{143}Nd/^{144}Nd$ ratio. In addition, the results from G224-2 show that Sm-Nd systematics are not affected by the presence hydrous alteration minerals such as uralite. This is evidence that the correlated variations of $^{143}Nd/^{144}Nd$ and $^{147}Sm/^{144}Nd$ ratios in these minerals represent an isochron rather than an accidental mixing line. The combined Ibra data give an age of 130 ± 12 m.y. and ϵ_{Nd} = 7.8 ± 0.2. This will be used as a reference isochron for comparison of other data from the Ibra section.

In order to determine whether there exist any variations in either the age or initial $^{143}Nd/^{144}Nd$ ratio we analyzed the gabbro OM251 which was collected in Wadi Fizh approximately 300 km NW from the Ibra section (see Figure 1). The plagioclase and clinopyroxene data points from this gabbro give an age of 100 ± 20 m.y. and an initial of ϵ_{Nd} = 7.6 ± 0.3 (Figure 4). This initial ratio is slightly lower than that obtained from the Ibra section, and the crystallization age appears to be about 30 m.y. younger (note, however, that the error bars on the two isochron ages overlap). This age difference, if substantiated, would imply a tectonic break, for example, a transform fault, with a large lateral offset. Such a structure conceivably might be located in the Samail gap (Figure 1).

Tilton et al. [1981] have dated plagiogranites along the entire length of the Oman Mountains by using the uranium lead technique on zicrons and found U-Pb ages which are virtually constant (94–98 m.y.) for the entire ophiolite. On the basis of these consistent results, *Tilton et al.* [1981] interpret the zircon ages as the time of igneous crystallization. Sm-Nd ages obtained from north of the Samail gap (Figure 1) agree with the zircon results. However east of the Samail gap, the Sm-Nd data from Ibra give consistently older (~30 m.y.) ages than the plagiogranites. Since all Sm/Nd and $^{143}Nd/^{144}Nd$ were determined from the same spiked solution for samples northwest of the Samail gap, K9 clinopyroxene was repeated using this same technique. The results of the second run are within experimental error the same as the aliquot data (Table 1). Note that the second run was performed on a new mineral separate, yet the Sm-Nd systematics did not change, thereby indicating the reliability of the data. The contrast between the two Ibra ages suggests that the U-Pb and Sm-Nd clocks are recording different events southeast of the Samail gap.

The geologic significance of the age discrepancy is not resolved. However, the internal consistency of both the U-Pb [*Tilton et al.*, 1981] and the Sm-Nd data indicates that extreme caution must be exercised when attaching a geologic inter-

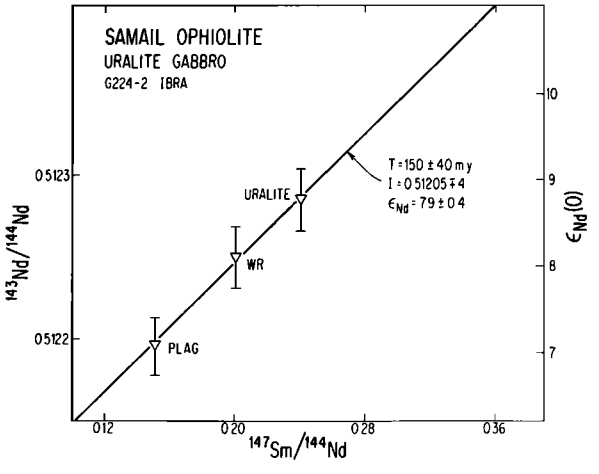

Fig. 3. Sm-Nd evolution diagram for the high-level uralite gabbro G224-2, from the Ibra section, Oman. The larger uncertainty in the age determination compared to the gabbro K9 is due to the smaller spread in $^{147}Sm/^{144}Nd$ ratios of the plagioclase and uralite. The uralitization process must have occurred close to the time of crystallization of the gabbro and does not appear to have disturbed the Sm-Nd systematics.

pretation to either of the ages. The zircon and Sm-Nd age data from the Blow-Me-Down massif, Bay of Islands, Newfoundland [*Mattinson*, 1976; *Jacobsen and Wasserburg*, 1979], illustrate this point. The Sm-Nd internal isochron ages of 508 ± 6 m.y. and 501 ± 13 m.y. for pyroxene gabbro agree with the upper intercept on the U-Pb concordia diagram in a discordia interpretation of the zircon data. Mattinson analyzed three separate zircon fractions (separated using magnetic and size characteristics) from the same plagiogranite and noted that each fraction was concordant within analytical uncertainty. This result is typical for young samples. If only one split from the entire zircon population had been analyzed, the zircon U-Pb age would have been 10–30 m.y. younger than Sm-Nd age from the same section. Because of the low zircon contents of the Oman plagiogranites it was possible to analyze only one fraction for each plagiogranite. Using this technique on such young samples prevents any assessment of possible dispersion along the concordia in a single plagiogranite, and thus the interpretation of the zircon ages as the time of primary igneous crystallization may be subject to question.

Sm-Nd Whole Rock Analyses of Basalts, Sheeted Dikes, Plagiogranite, and Harzburgite

Sm-Nd whole rock analyses were obtained from a plagiogranite (G224-3), sheeted dikes (G10, K1), and a basalt (G54) from the Ibra section. In addition, a calcite amygdule from the basalt G54 was also analyzed for Sm-Nd. From the $\delta^{18}O$ values and petrography these samples show varying degrees and conditions of alteration and metamorphism, ranging from zeolite to greenschist facies. With the exception of the basalt, only a single data point was obtained for each sample, and it is therefore not possible to calculate independently both the age and initial ratio for each sample. Therefore in Figure 5 these data are compared with the mineral isochron defined by the gabbros from Ibra. Apart from the sheeted dike K1, the data all lie within analytical error of the gabbro reference isochron. This is consistent with these samples having the same crystallization age (130 m.y.) and initial $^{143}Nd/^{144}Nd$ ratio. This can be seen from the ϵ_{Nd} values given in Table 1, which for an age of 130 m.y. range from 7.5 ± 0.4 to 8.3 ± 0.3 compared to ϵ_{Nd} = 7.8 ± 0.2 for the two Ibra gabbros. The plagiogranite G224-3, with ϵ_{Nd} = 8.2 ± 0.3, has a clear affinity with these rocks and must represent a later first or second

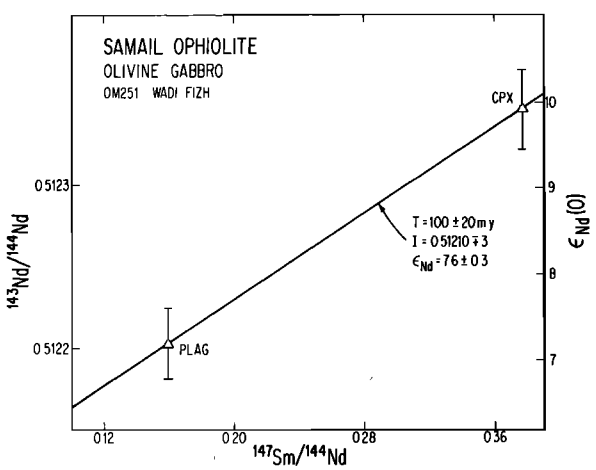

Fig. 4. Sm-Nd evolution diagram for the cumulate gabbro OM251, from Wadi Fizh, northern Oman (see Figure 1).

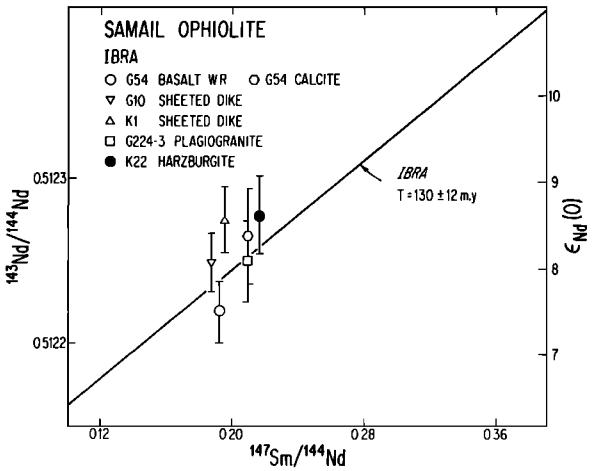

Fig. 5. Sm-Nd evolution diagram showing whole rock data for basalt, sheeted dikes, and plagiogranite from the Ibra section, Oman. With the exception of the sheeted dike K1 the data from the other samples are consistent with the same crystallization age and initial $^{143}Nd/^{144}Nd$ ratio as the gabbros from Ibra. The deviation of K1 indicates the presence of small but significant isotopic heterogeneities in the magma reservoirs. The tectonite harzburgite K22 is within analytical uncertainty of the Ibra reference isochron. This is consistent with the harzburgite being a cogenetic of the partial melting event which produced the rest of the ophiolite.

stage differentiate from the same type of oceanic magma source and cannot be a product of melting of any older continental basement.

The tectonized harzburgite K22 with ϵ_{Nd} = 8.3 ± 0.4 is also within analytical uncertainty of the Ibra reference isochron. This suggests that the harzburgite is genetically related to the rest of the ophiolite (i.e., cumulate gabbro and high level volcanics) and that the serpentization of the harzburgite has not disturbed the Sm-Nd system.

The Sm-Nd analysis of the diabase dike K1 does not overlap with the reference isochron. This cannot be explained by seawater alteration, as the more altered samples are consistent with the reference isochron. This small deviation of K1 could be due to variations in both initial $^{143}Nd/^{144}Nd$ ratio and the crystallization age. As it is unlikely that significant age differences exist within the same section, the deviation of K1 is most probably due to a variation in its initial $^{143}Nd/^{144}Nd$ ratio. For an age of 130 m.y. this corresponds to ϵ_{Nd} = 8.6 ± 0.4 for K1 compared to ϵ_{Nd} = 7.8 ± 0.2 for the Ibra gabbros and indicates the presence of small but significant isotopic heterogeneities in the magma reservoirs.

In an attempt to ascertain directly the Nd isotopic characteristics of the interacting fluid we analyzed a calcite amygdule from the basalt G54. The amygdule has ϵ_{Nd} = 8.1 ± 0.6 which is within error the same as the host basalt. While the solution that deposited the calcite was most likely derived from seawater with an initially negative ϵ_{Nd} value [*O'Nions et al.*, 1978; *Piepgras et al.*, 1979], the calcite gave an ϵ_{Nd} value which indicates that the final fluid must have obtained the Nd from the parent rock and not from seawater.

DISCUSSION

Implications of Sm-Nd

The presence in the Samail ophiolite of only small variations in the initial $^{143}Nd/^{144}Nd$ ratios from different localities and stratigraphic units appears to indicate a relatively uniform isotopic source regions. It is therefore useful to compare

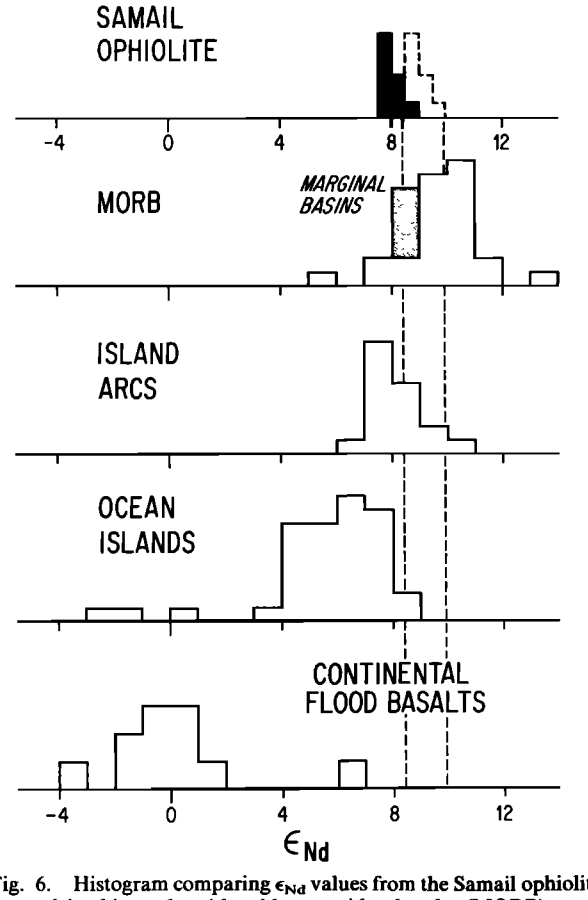

Fig. 6. Histogram comparing ϵ_{Nd} values from the Samail ophiolite measured in this study with midocean ridge basalts (MORB), marginal basins (Lau, Scotia Sea), island arcs, ocean islands, and continental flood basalts. The Samail ophiolite clearly has an oceanic affinity, although because of the overlap the Nd isotopic data by themselves cannot definitely distinguish among the various possible oceanic environments. The dashed lines show the ϵ_{Nd} values of the Samail ophiolite corrected for differential evolution relative to the bulk earth during the past 130 m.y. (see discussion).

these initial ratios with those found in young ocean ridge, ocean island, island arc, and continental basalts. In Figure 6, ocean ridge and island arc tholeiites have ϵ_{Nd} values which overlap, with ocean ridge tholeiites having a range of +7 to +13 and island arcs ranging from +7 to +10. These values [*DePaolo and Wasserburg*, 1976*a*, 1977; *O'Nions et al.*, 1977; *Hawkesworth et al.*, 1977; *Richard et al.* 1976] are distinctive from the ocean island range of ~+4 to +8 [*O'Nions et al.*, 1977; *DePaolo and Wasserburg*, 1977]. The ϵ_{Nd} for oceanic rocks are very different from young continental tholeiitic basalts with have $\epsilon_{Nd} \sim 0$ [*DePaolo and Wasserburg*, 1976*a*; *Carlson et al.*, 1978] and older continental crust having $\epsilon_{Nd}(0) \ll 0$ [*DePaolo and Wasserburg*, 1976*a*; *McCulloch and Wasserburg*, 1978]. The Samail ophiolite with $\epsilon_{Nd} = 7.8$ clearly has an oceanic affinity lying in the lower limit of the island arc and ocean ridge basalt range and the uppermost limit of the ocean island range. Because of the overlap of ϵ_{Nd} values from different tectonic settings shown on Figure 6 the Nd isotopic data cannot distinguish among various possible genetic models such as midocean ridge, back arc basin, ocean island, or island arc origin for the Samil ophiolite. However, the lack of light REE enriched samples and alkalic volcanism usually associated with ocean island and island arc environments suggest that the most reasonable scenario for its formation is in an ocean basin.

The value of $\epsilon_{Nd} = 7.8$ in the Samail ophiolite is somewhat lower than 'typical' MORB with $\epsilon_{Nd} \approx 10$. This may be due to the older age of the Samail ophiolite compared to the zero age basalts plotted in Figure 6, or it may simply reflect the overall variability present today in ocean ridge basalts. The dispersion in ϵ_{Nd} of modern day oceanic basalts is to some extent correlated with chemistry. Alkalic rocks generally have lower ϵ_{Nd} values than MOR tholeiites [*Carlson et al.*, 1978]. However, several oceanic tholeiites with relatively low ϵ_{Nd} values in the range of +7.0 to 8.5 have also been found, for example, in the Atlantic (113152 [*DePaolo and Wasserburg*, 1976*b*], and ARP75 [*Richard et al.*, 1976]) and Pacific (BD17-1 [*DePaolo and Wasserburg*, 1976*b*]) oceans. These samples do not appear to be chemically or tectonically distinctive, although the isotopic data indicate an origin from a less depleted source reservoir. Tectonically distinctive oceanic settings which may be modern day analogues of the environment in which the Samail ophiolite was formed are the Lau marginal basin and Scotia Sea back arc. The ϵ_{Nd} values from these two areas [*Hawkesworth et al.*, 1977; *Carlson et al.*, 1978] are shown in Figure 6 and define a relatively narrow range in ϵ_{Nd} of from 8.1 to 9.0. These ratios are also somewhat low compared to normal MORB samples and are very similar to the Samail ophiolite.

To some extent the slightly lower ϵ_{Nd} value of the Samail ophiolite compared to typical oceanic crust is due to the evolution of $^{143}Nd/^{144}Nd$ in the oceanic mantle reservoirs during the past 130 m.y. To correct for this evolution, an estimate of the $^{147}Sm/^{144}Nd$ ratio in the Samail ophiolite source reservoir is required. This can be obtained by assuming that the composite of the cumulate gabbros, diabase dikes, and pillow basalts represents the primary unfractionated magma. From the Samail ophiolite data we estimate that this magma had Nd ~ 4 ppm and Sm ~ 1.6 ppm. This corresponds to $^{147}Sm/^{144}Nd \sim 0.24 \pm 0.02$. As Nd and Sm are strongly partitioned into the liquid during partial melting, this is also probably a reasonable estimate for the source reservoir. For this value of $^{147}Sm/^{144}Nd$ the Samail source reservoir evolves by ~0.6 ϵ_{Nd} units per 100 m.y. and would today have $\epsilon_{Nd} \sim 8.7$. Thus the ϵ_{Nd} value of the Samail ophiolite would now only be about ~1 ϵ_{Nd} unit below the center of the MORB distribution and is there-

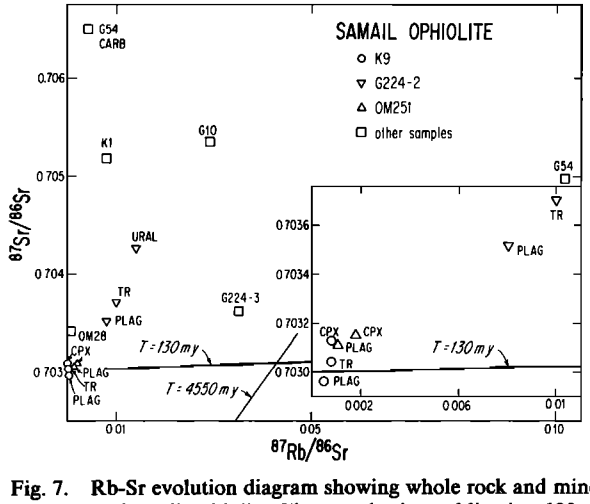

Fig. 7. Rb-Sr evolution diagram showing whole rock and mineral data from the Samail ophiolite. The near-horizontal line is a 130-m.y. isochron and the steeper line is for an isochron of 4550 m.y. The lack of correlation between $^{87}Rb/^{86}Sr$ and $^{87}Sr/^{86}Sr$ and the high $^{87}Sr/^{86}Sr$ is attributed to contamination by seawater.

fore fully consistent with a MORB affinity. It is also noted that for the MORB source reservoir to evolve in a single stage from $\epsilon_{Nd} = 0$ to the modern day value of $\epsilon_{Nd} = +10$ requires, for $^{147}Sm/^{144}Nd = 0.24$, at time interval of 1.7 eons. This result is similar to the single stage differentiation ages obtained by Pb-isotope studies [*Church and Tatsumoto*, 1975; *Sun et al.*, 1975].

The relationship of the basal peridotites to the rest of the ophiolite sequence has been obscure due to the effects of deformation and post-emplacement alteration which have strongly modified the primary geologic structures and relationships. Various hypotheses summarized by *Coleman* [1977] have considered the harzburgite as a (1) cogenetic lowermost cumulate, (2) older accidental mantle substrate with is not petrogenetically linked to the rest of the ophiolite, or (3) a cogenetic refractory residue remaining from the partial melting which produced the rest of the ophiolite. The initial Nd value of $\epsilon_{Nd} = 8.3 \pm 0.4$ for the tectonized harzburgite K22 is within error the same as the rest of the ophiolite. This result, together with the low trace element concentrations, supports the third hypothesis.

There is, however, conflicting evidence from the U-shaped (convex downward chondrite normalized) rare earth element (REE) patterns which have been observed in the Samail harzburgite [*Pallister and Knight*, 1981] and a number of other peridotites [*Allegre et al.*, 1973; *Kay and Senechal*, 1976; *Frey*, 1969; *Suen et al.*, 1979]. On the basis of U-shaped REE patterns in harzburgite and dunite from Newfoundland, *Suen et al.* [1979] have concluded that the tectonite peridotite could not be related to the overlying oceanic crust by a simple partial melting event. Their argument against a cogenetic origin for the harzburgite is that residues of light REE (LREE) depleted MORB should also exhibit LREE depletion. The argument depends upon the choice of crystal-liquid partition coefficients for olivine and orthopyroxene. Natural olivines from meteorites and from peridotite [*Schetzler and Bottino*, 1971; *Masuda*, 1968; *Frey*, 1969] may exhibit U-shaped REE patterns. Combining natural olivine-orthopyroxene partition coefficient data from *Frey* [1969] with experimentally determined orthopyroxene-liquid data reviewed by *Irving* [1978] suggests that residual harzburgites can have U-shaped patterns because olivine dominates the light REE and orthopyroxene dominates the heavy REE. A cumulate dunite measured by *Suen et al.* [1979] (which on geologic grounds crystallized from the same melts that produced LREE depleted diabases [*Malpas*, 1978]) has a U-shaped pattern. If we assume that REE partitioning between cumulate and liquid is the same as partitioning between residue and liquid, then a cogenetic residue of harzburgite should also exhibit such a pattern but at lower concentrations.

The harzburgite REE concentrations are lower than expected from simple one-stage partial melting and are a consequence of the plumbing system that delivers melts to the surface. Two processes enrich the overall REE contents in ophiolitic diabases and by analogy in seafloor basalts: (1) open system fractionation in crustal magma chambers driven by periodic intrusion and mixing into the chamber of primitive magma [*Stern*, 1979; *Pallister and Knight*, 1981] and (2) fractionation of olivine during ascent of the primary melt bodies through the upper mantle [*Hopson et al.*, 1981]. The second process is a consequence of the fact that enstatite is not an early liquidus phrase at low pressure for any MORB compositions—confirmed experimentally by *Green et al.* [1979] and *Stolper* [1980] and in the Samail ophiolite [*Hopson et al.*, 1981; Pallister and Hopson, 1980]. The implication of this relationship is that above depths of 30 km [*Stolper*, 1980] all harzburgite-melt contacts become sites of reaction between ascending melts and their host rocks which are not in magmatic equilibrium. The upward migration and reaction of the melts with the harzburgite is manifested in the Samail peridotite as cross-cutting dunite bodies [*Boudier and Coleman*, 1981]. Using field estimates of the amount of dunite present in the Samail peridotite, fractionation of olivine during ascent may enrich the REE of the melt by as much as a factor of 2.

The former process documented by *Pallister and Knight* [1981] has enriched the overall REE concentrations of Samail melts by factors up to five. In samples K9 and OM251 a 4-fold enrichment is observed. These combined crustal and upper mantle processes may lead to order of magnitude enrichments of overall bulk REE between initial melt segregation and crystallization. Therefore any trace element concentration arguments concerning genetic relationships between rocks such as the harzburgites and diabases are subject to postseparation processes which cannot be constrained without other petrologic data (usually not available with seafloor samples). In contrast, the Nd isotope data which are independent of the vagaries of the plumbing system see through this history and thus provide a more straightforward test of the primary relationship between harzburgite and the overlying oceanic crust.

The partial melting event which produced the harzburgite residue is unlikely to be exactly contemporaneous with the crystallization of the immediately overlying pile of cumulate gabbros, sheeted dikes, and pillow lavas. The following sequence is suggested. Partial melting of an already LREE depleted source material (lherzolite) at depths of 60 to 70 km [*Green et al.*, 1979] is followed by melt segregation. The residual harzburgite ascends with a rate constrained by the spreading rate to form the basement of the cumulate gabbros and basaltic suites. For a half spreading rate of 1 cm/yr the harzburgite would take ~6 m.y. to rise from the partial melting zone. In contrast, the magma produced during this partial melting would rise much more rapidly at the rate of ~1 km/yr, otherwise the melt would crystallize before reaching the surface [*Marsh*, 1979]. Thus for the conservative spreading rate used in this example the formation of the harzburgite residue probably occurred, at most, 6 m.y. prior to the crystallization of the immediately overlying magmatic suite. This time difference is not resolvable with the present Sm-Nd data. Thus within the analytical uncertainities the harzburgite and overlying magmatic sequences are considered to be cogenetic.

Comparison of Rb-Sr and Sm-Nd

The most obvious contrast between the Sr and Nd isotopic systems is the larger variability of the $^{87}Sr/^{86}Sr$ ratios ranging from 0.70296 ($\epsilon_{Sr} = -19.7$) to 0.70650 ($\epsilon_{Sr} = +30.5$) compared to a range in ϵ_{Nd} of from only 7.5 to 8.6. The lowest $^{87}Sr/^{86}Sr$ ratios are found in the plagioclase separates from the layered cumulate gabbros K9 and OM251. In K9 the plagioclase has an $^{87}Sr/^{86}Sr$ ratio of 0.70296 ± 2. However, the coexisting clinopyroxene has a distinctly higher value of 0.70313 ± 3. In Figure 7 reference isochrons of 130 and 4550 m.y. are shown. A line connecting the clinopyroxene and plagioclase from K9 gives an impossibly old age of >4.5 eons. In the high-level gabbro G224-2 there is a similar disparity between the plagioclase and uralite. The uralite has an $^{87}Sr/^{86}Sr$ ratio of 0.70426 ± 3 compared to 0.70352 ± 4 for the coexisting plagioclase. These isotopic variations cannot be accounted for

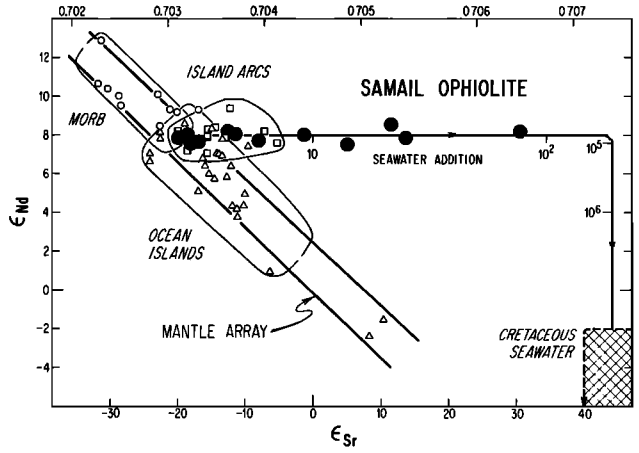

Fig. 8. The ϵ_{Nd} and ϵ_{Sr} values for the Samail ophiolite (solid). The arrows indicate the effect of contamination with Cretaceous seawater for different water/rock ratios and show that $W/R > 10^5$ is required before ϵ_{Nd} values are affected. The ϵ_{Nd} and ϵ_{Sr} values of uncontaminated samples plot within the 'mantle array' and are consistent with derivation from a MORB source region.

by radiogenic decay since crystallization. Instead, this isotopic relationship between the coexisting mineral phases indicates partial exchange with a source of high $^{87}Sr/^{86}Sr$. The enrichment in $^{87}Sr/^{86}Sr$ is more pronounced in the clinopyroxene and uralite and is anticipated as they have a factor of 5 lower Sr concentration than the plagioclase. This enrichment is also consistent with the petrography as the uralite is clearly an alteration product and the clinopyroxene contains ~5% secondary hornblende. These results are in distinct contrast to Sm-Nd, where all mineral phases plot on a 130 m.y. isochron.

The highest $^{87}Sr/^{86}Sr$ ratios found in the Samail ophiolite are in the upper sequences consisting of basalts, sheeted dikes, and plagiogranites. The higher $^{87}Sr/^{86}Sr$ ratios in these rocks is consistent with a greater degree of exchange with seawater having a high $^{87}Sr/^{86}Sr$ ratio. In an attempt to determine the $^{87}Sr/^{86}Sr$ ratio in seawater we analyzed a calcite amygdule from the basalt OMG54. This has $^{87}Sr/^{86}Sr = 0.7065$ which is significantly higher than that found for any of the igneous rocks and may be compared to 0.7076 estimated for Cretaceous seawater [*Peterman et al.*, 1970; *Veizer and Compston*, 1974]. These observations are clearly consistent with hydrothermal interaction with seawater. The slightly lower ratio in the carbonate amygdule compared to Cretaceous seawater is probably due to the lowering of $^{87}Sr/^{86}Sr$ in the fluid by interaction with the rock. There is also an approximate correlation between high $^{87}Sr/^{86}Sr$ and stratigraphic height (see Figure 11) which suggest that water/rock increased upward in the section.

Because of the overprinting of rock Sr with seawater Sr it is not possible to determine unambiguously the primary magmatic $^{87}Sr/^{86}Sr$ ratio in these rocks. An upper limit is given by the lowest $^{87}Sr/^{86}Sr$ value of 0.70296 found in the plagioclase from the gabbro K9. This may be close to its magmatic value as the coexisting clinopyroxene with a lower Sr concentration has only a slightly greater $^{87}Sr/^{86}Sr$ ratio. The $^{87}Sr/^{86}Sr$ ratios in the clinopyroxene and plagioclase from the gabbro OM251 also have very different Sr concentrations but have the same $^{87}Sr/^{86}Sr$ ratio within error and should thus also represent a primary value. The difference between the plagioclase separates from K9 and OM251 of 0.70296 ± 2 and 0.70311 ± 5 could therefore indicate a small but real difference in the $^{87}Sr/^{86}Sr$ ratios of these samples and apparently of the original magmas from which they crystallized. This suggests that small $^{87}Sr/^{86}Sr$ mantle isotopic heterogeneities may have been preserved during the formation of the Samail ophiolite because the same effect is also apparent in the Nd isotopic data (Table 1). In fact these two samples OM251 and K9 plot right on the MOR correlation line in the ϵ_{Sr}-ϵ_{Nd} diagram of Figure 8.

The importance of distinguishing between seawater alteration effects and mantle isotopic variations is illustrated in the Rb-Sr isochron diagram of Figure 7. In this figure, seawater alteration has produced an approximate correlation between Rb/Sr and $^{87}Sr/^{86}Sr$. If interpreted literally, this correlation would imply that Rb/Sr heterogeneities have existed for at least several billion years in the mantle reservoirs of the Samail ophiolite. Similar correlations and interpretations have been suggested in other ophiolites [*Peterman et al.*, 1971], oceanic basalts [*Brooks et al.*, 1976; *Hedge*, 1978], and ocean islands [*Sun and Hanson*, 1975; *Duncan and Compston*, 1976; *Whitford et al.*, 1977]. Although some of these correlations are undoubtedly due to mantle features, the ^{18}O and Sr data from the Samail ophiolite indicate that in this case the Rb/Sr-$^{87}Sr/^{86}Sr$ correlation is clearly an artifact of seawater alteration.

A useful criterion to distinguish between isotopic variations due to either primary magmatic or seawater alteration effects is the ϵ_{Nd}, ϵ_{Sr} diagram. In Figure 8 the ϵ_{Nd} and ϵ_{Sr} values from the Samail ophiolite are shown. They have an origin at the mantle correlation line [*DePaolo and Wasserburg*, 1976*b*; *O'Nions et al.*, 1977] and form a horizontal trajectory to the higher ϵ_{Sr} values. Although this general effect has been observed by previous workers [*DePaolo and Wasserburg*, 1977; *O'Nions et al.*, 1977], the present results provide a spectacular example of how the Nd isotopic composition is unaffected by seawater contamination, while the Sr composition is shifted drastically. It is illustrative to compare the observed ϵ_{Nd}, ϵ_{Sr} values with those calculated for contamination of oceanic crust by Cretaceous seawater. Assuming a simple closed system model for mixing of Sr and Nd in seawater with oceanic crust, mass balance between the initial and final products gives:

$$W\epsilon_{water}{}^{i} + r\epsilon_{rock}{}^{i} = W\epsilon_{water}{}^{f} + r\epsilon_{rock}{}^{f} \quad (3)$$

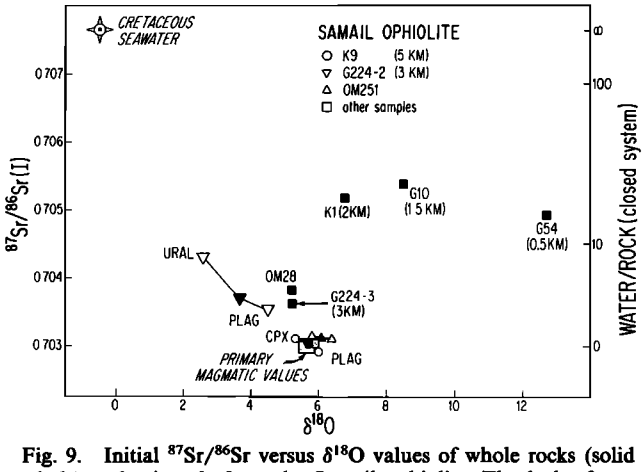

Fig. 9. Initial $^{87}Sr/^{86}Sr$ versus $\delta^{18}O$ values of whole rocks (solid symbols) and minerals from the Samail ophiolite. The lack of any simple correlation between $^{87}Sr/^{86}Sr$ and $\delta^{18}O$ indicates different temperatures (see Figure 10) of hydrothermal interaction of seawater and a complex history for the seawater-derived fluid. W/R ratios are calculated assuming that initial Cretaceous seawater had $^{87}Sr/^{86}Sr = 0.7076$, Sr = 8 ppm, and the initial rocks had $^{87}Sr/^{86}Sr = 0.703$, Sr = 160 ppm.

where w and r are the atomic proportions of Nd or Sr in the water and rock systems respectively and $\epsilon_{rock}{}^{i}$ is the initial ϵ_{Nd} or ϵ_{Sr} value in the rock before exchange, $\epsilon_{rock}{}^{f}$ is the final modified rock ϵ_{Nd} or ϵ_{Sr} value, $\epsilon_{water}{}^{i}$ is the initial ϵ_{Nd} or ϵ_{Sr} value in water before exchange, and $\epsilon_{water}{}^{f}$ is the modified water ϵ_{Nd} or ϵ_{Sr} value. For equilibrium exchange of water and rock, $\epsilon_{water}{}^{f} = \epsilon_{rock}{}^{f}$, and from (3) the water/rock ratio by weight is given by

$$\frac{W}{R} = \left(\frac{\epsilon_{rock}{}^{f} - \epsilon_{rock}{}^{i}}{\epsilon_{water}{}^{i} - \epsilon_{rock}{}^{f}}\right)\frac{C_{rock}{}^{i}}{C_{water}{}^{i}} \quad (4)$$

where $C_{rock}{}^{i}$ is the concentration of Sr or Nd in initial rock and $C_{water}{}^{i}$ is the concentration of Sr or Nd in seawater.

For Sr the parameters used in this equation are $\epsilon_{rock}{}^{i} = -20$, $\epsilon_{water}{}^{i} = +47$ [*Peterman et al.*, 1970], and $C_{water}{}^{i} = 8$ ppm [*Goldberg*, 1965]. The $\epsilon_{rock}{}^{f}$ values are given in Table 1. It is assumed that the initial Sr concentration in the rock ($C_{rock}{}^{i}$) is the same as the final measured concentration (Table 2). For Nd the parameters used in (4) are $\epsilon_{rock}{}^{i} = +8.0$, $\epsilon_{water}{}^{i} = -7$, and $C_{water}{}^{i} = 2.8 \times 10^{-6}$ ppm [*Piepgras et al.*, 1979]. The $C_{rock}{}^{i}$ and $\epsilon_{rock}{}^{f}$ values are given in Tables 1 and 2.

Using (4) and the Sr and Nd parameters, the ϵ_{Nd} and ϵ_{Sr} values in the rock resulting from mixing of different proportions of seawater with oceanic crust have been calculated. The ϵ_{Nd}-ϵ_{Sr} mixing line is shown in Figure 8 together with the water/rock ratios calculated for rock Sr and Nd concentrations of 180 and 10 ppm, respectively. From Figure 9 it can be seen that the ϵ_{Nd} values are far less sensitive to seawater contamination than the ϵ_{Sr} values. This is due to the significantly lower concentration of Nd in seawater of 2.8×10^{-6} ppm compared to 8 ppm for Sr. For example, the Sr data indicate that the sample with the highest water/rock ratio is the diabase dike K1 with $W/R = 43$ (Table 3). Using the Sr water/rock ratio for K1 and solving for $\epsilon_{rock}{}^{i}$ show that a $W/R = 43$ causes an insignificant change of $\epsilon_{Nd} = -0.0001$. To produce a measurable shift in ϵ_{Nd} of 0.5, a water/rock ratio of $W/R = 1.6 \times 10^{5}$ would be required. Thus relative to the most altered rock, an increase in the water/rock ratio of $\sim 4 \times 10^{3}$ would be required before seawater contamination would measurably change the ϵ_{Nd} values. A detailed analysis of the effects of seawater interaction using ϵ_{Sr} and $\delta^{18}O$ variations will be given in the following section.

Comparison of $^{87}Sr/^{86}Sr$ and $\delta^{18}O$

It has already been shown that $^{87}Sr/^{86}Sr$ and $\delta^{18}O$ values are sensitive to hydrothermal alteration. The effects of alteration on both these systems is shown in the initial $^{87}Sr/^{86}Sr$, $\delta^{18}O$ diagram of Figure 9. In this figure there appears to be at least two distinct trends which are centered about the primary values of $\delta^{18}O \approx +6$ and $^{87}Sr/^{86}Sr \approx 0.7030$. The most obvious trend is the approximate inverse correlation corresponding to depleted $\delta^{18}O$ and high $^{87}Sr/^{86}Sr$ ratios. The second, less distinctive, feature is the association of heavy $\delta^{18}O$ values with high $^{87}Sr/^{86}Sr$ ratios in the sheeted dikes and basalt. In an attempt to understand these features we will now consider simple models for the exchange of Sr and O with seawater.

TABLE 3. Sr Water/Rock Ratios for Closed and Open Systems, Ibra Section

Sample	W/R	
	Open System	Closed System
G54	11.6	14.8
G10	14.0	20.2
K1	31.1	43.5
G224-3	3.3	3.6
G224-2	4.2	4.5
K9	0.5	0.5

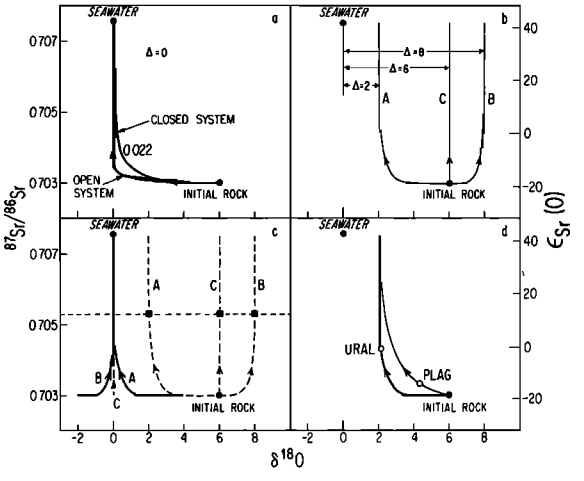

Fig. 10. (*a*) The ϵ_{Sr} and $\delta^{18}O$ mixing lines for $\Delta = 0$ and $C = 0.22$. The closed system curve is calculated using (8) and maps out the locus of ($\delta^{18}O$, ϵ_{Sr}) for systems with fixed W/R and water recirculation. The open system curve allows each packet of water to pass through the rock only once; thus no recirculation is permitted. In areas where hot spring activity occurs, such as the Galapagos rift [*Corliss et al.*, 1979], the open system equation applies. The 'one pass' curve is calculated by substituting the expression for open system water/rock (equation (9)) into (7). For Δ and C fixed, the natural systems lie between the two curves. (*b*) The ϵ_{Sr} and $\delta^{18}O$ values in the rock for $C = 0.022$ and $\Delta = 2$ (line A), $\Delta = 6$ (line C), and $\Delta = 8$ (line B). For $\Delta = 6$, which corresponds to a temperature of $\sim 300°C$, there can be shifts in ϵ_{Sr} without any change in $\delta^{18}O$. (*c*) The ϵ_{Sr} and $\delta^{18}O$ values in water for $\Delta = 2$, $\Delta = 6$, and $\Delta = 8$ (solid lines) are given by $\delta^{18}O_{water}{}^{f} = \delta^{18}O_{rock}{}^{f} - \Delta$ and $\epsilon_{rock}{}^{f}$. For $\Delta < 6$, which corresponds to temperature >300°C, seawater will be enriched in ^{18}O as long as the water/rock ratio is small. For $\Delta > 6$ (<300°C) ^{18}O-depleted waters will be produced. The dashed lines show the ϵ_{Sr} and $\delta^{18}O$ values in the rock (from Figure 10*b*). The horizontal dashed line illustrates how the combined strontium and oxygen data can be used as a geothermometer for hydrothermal interactions if the W/R obtained from the $^{87}Sr/^{86}Sr$ ratios is used to solve the oxygen W/R equation for $\Delta(T)$. (*d*) Example of mixing lines consistent with ϵ_{Sr} and $\delta^{18}O$ values in the uralite gabbro.

Let us consider a simple closed system model for the exchange of Sr and O with seawater as has already been discussed for Sr and Nd. Using this model, the water/rock ratio (by weight) calculated using $\delta^{18}O$ variations is given by *Taylor* [1974]:

$$\frac{W}{R} = \left(\frac{\delta_{rock}{}^{f} - \delta_{rock}{}^{i}}{\delta_{water}{}^{i} - (\delta_{rock} - \Delta)}\right)\frac{C^{i}O_{rock}}{C^{i}O_{water}} \quad (5)$$

This equation is identical to that used for Sr, apart from the temperature dependent fractionation factor Δ. Let us now assume that only a particular fraction of the rock exchanges oxygen with seawater. This may, for example, be the case for rocks with different modal proportions of easily exchanged minerals such as feldspar. The effective water/rock ratio (W/R(effective)) is then given by

$$\frac{W}{R}\text{(effective)} = \frac{W}{R} \times \frac{1}{q} \quad (6)$$

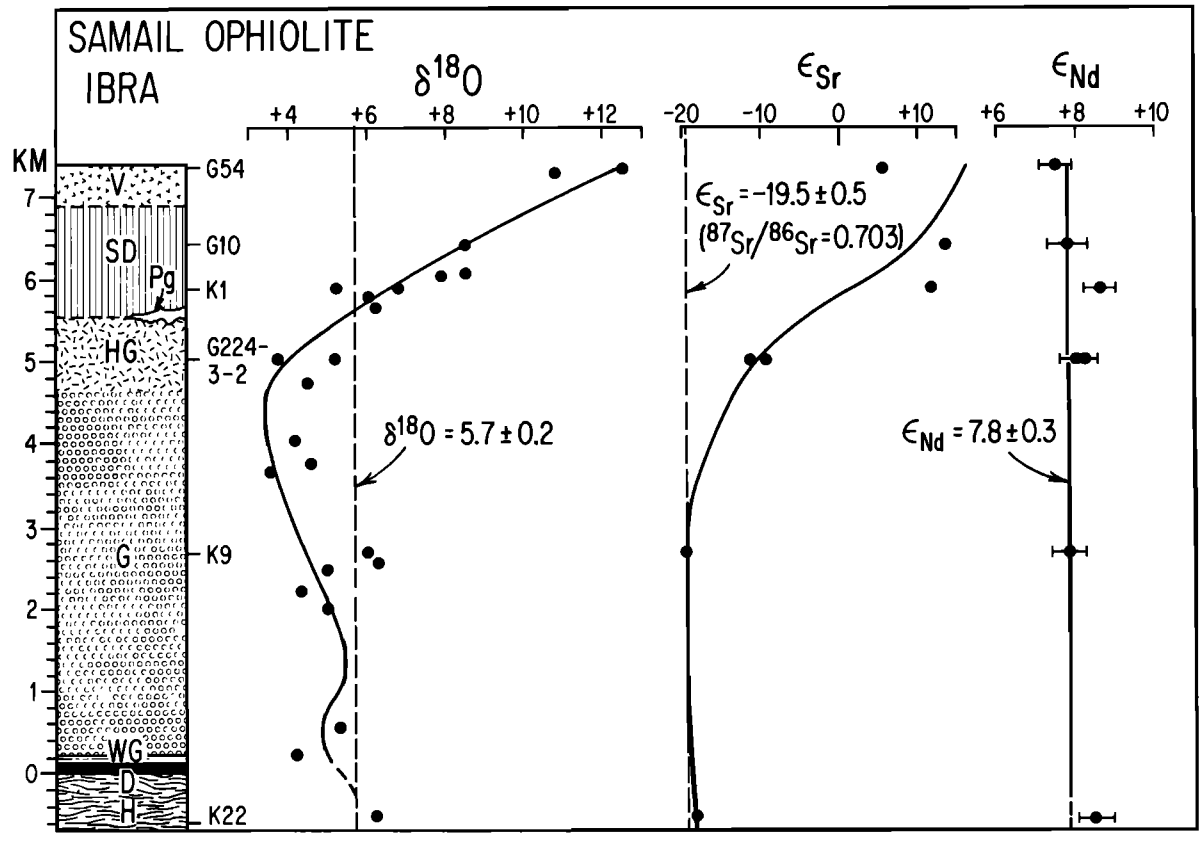

Fig. 11. The $\delta^{18}O$, ϵ_{Sr}, and ϵ_{Nd} values from a composite profile through the Samail ophiolite, Ibra section. The ophiolite section was compiled from the geologic map of *Bailey et al.* [1980]. The symbol V = pillowed volcanic, SD = sheeted dikes, Pg = plagiogranite, HG = high-level gabbro, G = cumulate gabbro, WG = interlayered wehrlite and gabbro, D = dunite, and H = harzburgite. The plagiogranites and differentiated high-level gabbros are the last intrusive rocks to crystallize. It can be seen that the ϵ_{Nd} values are, in general, within error of the primary magmatic value of ϵ_{Nd} = 7.8. In contrast, the $\delta^{18}O$ [from *Gregory and Taylor*, 1981] and ϵ_{Sr} values show large deviations from their primary magmatic values of $\delta^{18}O$ = 5.7 and ϵ_{Sr} = −19.5. These large variations in $\delta^{18}O$ and ϵ_{Sr} are a consequence of hydrothermal interaction of seawater. The isotopic characteristics of the Samail ophiolite may be similar to those in oceanic crust undergoing subduction in present-day ocean basins.

where q is the fraction (by weight) of rock that exchanged with seawater. A similar equation can also be written for the Sr water/rock ratio, where, in this case, let us assume that different fractions of the rock, q' exchanged with seawater. Therefore the relationship between the Sr and O water/rock ratios is given by

$$\frac{W}{R}(\mathrm{Sr})\,\frac{1}{q'} = \frac{W}{R}(\mathrm{oxygen})\,\frac{1}{q} \tag{7}$$

Using this relationship, (4) and (5) can now be combined to give

$$\frac{\epsilon_{\mathrm{rock}}{}^{f} - \epsilon_{\mathrm{rock}}{}^{i}}{\delta_{\mathrm{rock}}{}^{f} - \delta_{\mathrm{rock}}{}^{i}} = \left(\frac{\epsilon_{\mathrm{water}}{}^{i} - \epsilon_{\mathrm{rock}}{}^{f}}{\delta_{\mathrm{water}}{}^{i} - (\delta_{\mathrm{rock}}{}^{f} - \Delta)}\right) \times C \tag{8}$$

where

$$C = \frac{C^{\mathrm{Sr}}{}_{\mathrm{water}}/C^{\mathrm{O}}{}_{\mathrm{water}} \times q'/q}{C^{\mathrm{Sr}}{}_{\mathrm{rock}}/C^{\mathrm{O}}{}_{\mathrm{rock}}}$$

An example of a mixing line using (7) is shown in Figure 10*a* for Δ = 0. It can be seen that the mixing line is a hyperbola with the curvature determined by the constant C. For $q'/q = 1$ and using average concentrations of Sr and O in the rock and seawater, C = 0.022 in both the closed and open system curves shown in Figure 10*a*. Using this arbitrary value of C, the effect of changing the oxygen water/rock fractionation factor from Δ = +2 to Δ = +6 or +8 is shown in Figure 10*b*. The value of Δ depends on the temperature of exchange and is given by (2). Thus in an environment with changing exchange temperatures no simple correlation of $\delta^{18}O$ and $^{87}Sr/^{86}Sr$ would be expected. In fact, for Δ = 6 corresponding to a temperature of ~250°C there can be changes in $^{87}Sr/^{86}Sr$ without any change in the $\delta^{18}O$ (Figure 10*b*).

For $\Delta \neq 0$ the $\delta^{18}O$ value of the water is different from the $\delta^{18}O$ value of the rock, being related by $\Delta = \delta_{\mathrm{rock}}{}^{f} - \delta_{\mathrm{water}}{}^{f}$. The curves which map the water compositions are shown in Figure 10*c* for the different Δ values. In Figure 10*c*, for small W/R ratios (<3) when $\Delta < 6$, the final water which equilibrates with rock will be enriched in $\delta^{18}O$ (i.e., $\delta^{18}O_{\mathrm{water}}{}^{\mathrm{final}} > 0$) and for $\Delta > 6$, the water will be depleted. Subsequent interaction of this exchanged water will result in another set of mixing curves. Also, in Figure 10*c* the $^{87}Sr/^{86}Sr$ value can be used independently to assess the water/rock ratio. Then either the temperature of equilibration or the final fluid composition can be in principle calculated from (8). Using this reasoning on sample G10 (Figure 9) exhibiting a greenschist assemblage suggests that diabase G10 equilibrated with a seawater-derived fluid which had been exchanged and enriched by at least 2‰ over its initial value. Evidence has been found in the diabase dikes for exchange with ^{18}O-enriched water [*Gregory and*

Taylor, 1981], indicating that this water has had a history of high temperature (>300°C) exchange.

In Figure 10*d*, mixing lines are shown which could account for the Sr isotopic disequilibrium observed for example between the plagioclase and uralite in the gabbro G224-2. The mixing lines are different for each mineral as they have different Sr concentrations and presumably different exchange rates (i.e., different values of q'/q). As the factor q'/q is unknown, the mixing lines that are shown are arbitrary, but they qualitatively account for the observed $^{87}Sr/^{86}Sr$ and $\delta^{18}O$ values in the minerals of G224-2.

The above calculations were based on a closed system model which assumes continuous recirculation and cyclic reequilibration of the water with the rock. However, some of the heated water will be lost from the system, for example, by escape to the ocean. In the extreme open system case in which each increment of water makes only a single pass through the system the integrated water/rock ratio is given by the equation from *Taylor* [1977]:

$$\frac{W}{R}\left(\begin{matrix}\text{open}\\ \text{system}\end{matrix}\right) = \frac{C_{\text{rock}}^{\,i}}{C_{\text{water}}^{\,i}} \ln\left[\frac{C_{\text{water}}^{\,i}}{C_{\text{rock}}^{\,i}}\frac{W}{R}\left(\begin{matrix}\text{closed}\\ \text{system}\end{matrix}\right) + 1\right] \quad (9)$$

Water/rock ratios calculated from the Sr data and using both open and closed system models are tabulated in Table 3. The W/R ratios are lower in the gabbros than in the upper sequence. In addition, since the concentration constant in (9) is $\ll 1$, both the open and the closed system models give similar results (Table 3 and Figure 10*a*) except for large values of W/R. However, both of these models only give minimum values of W/R because an appreciable volume of water may move through fractures in the rocks without exchanging.

From this discussion it is apparent that the production of water with $\delta^{18}O > 0$ results from fluid-rock interaction at high temperatures (i.e., with $\Delta < 6$) in an environment with a low water-rock ratio such as in the gabbro section. This implies that the $\delta^{18}O$ effects in the sheeted dikes were produced by reaction with seawater already enriched in ^{18}O, by exchange with the underlying gabbros at higher temperature as suggested by *Gregory and Taylor* [1981]. This ^{18}O-shifted fluid would also presumably be shifted in $^{87}Sr/^{86}Sr$ (~0.704 indicated by uralite from G224-2) and may not have affected the diabases already enriched in ^{87}Sr during alteration over the ridge axis. As stated above, this implies that there are at least two temperature and spatial regimes where exchange of oxygen and Sr occurs. The first is at the ridge axis above the magma chamber where fluid path lines do not cross the diabase-magma contact. It is in this environment that ^{18}O-depleted rocks and $^{87}Sr/^{86}Sr$ enriched rocks would be produced during reaction and exchange with large volumes of seawater. Subsequently, with continued production of oceanic crust these rocks are transported away from the ridge into a cooler regime at the distal edges of the magma chamber where interaction between isotopically shifted fluids and the diabases occurs. A high ^{18}O fluid discharges from a second hydrothermal system which operates under the wings of the ridge magma chamber. This fluid imposes an ^{18}O enrichment upon the diabases which masks the earlier ridge axis oxygen exchange without appreciably affecting the Sr isotope ratios. This 'hydrothermal reworking' of oceanic crust may also explain the generally more altered nature of ophiolite pillow basalts and diabases compared to those dredged from ocean ridges.

SUMMARY AND CONCLUSIONS

1. In this study we have established the crystallization age of the Samail ophiolite by obtaining Sm-Nd mineral isochrons from gabbros. The gabbros from the southern part of the ophiolite in Ibra give an age of 128 ± 20 m.y. and 150 ± 40 m.y., while a gabbro from Wadi Fizh in the northern part of Oman gives a somewhat younger age of 100 ± 20 m.y. These results show that the Sm-Nd technique can be used to determine crystallization ages of relatively young mafic rocks.

2. The initial $^{143}Nd/^{144}Nd$ ratio of gabbros, plagiogranite, diabase dikes, and a basalt from the Samail ophiolite have a narrow range in ϵ_{Nd} of from 7.6 to 8.6 (Figure 11). This indicates derivation from a relatively uniform reservoir that has been depleted in the LREE for at least a billion years or more. The Samail ophiolite ϵ_{Nd} values are also within the range expected for Cretaceous MORB and therefore clearly indicate an oceanic affinity. An oceanic origin is also indicated by the lead isotopic studies of *Chen and Pallister* [1981].

3. The tectonized harzburgite has $\epsilon_{Nd} = 8.3$, which is the same as the overlying cumulate gabbros, sheeted dikes, and pillow basalts. This result, together with its low trace element concentrations, is consistent with the harzburgite being a cogenetic residue from partial melting event which produced the overlying magmatic sequences. However, considering the complexity and heterogeneous character of the peridotite in the Samail ophiolite [*Boudier and Colemen*, 1981], generalization of this result must await a more complete characterization of the peridotite.

4. In contrast to the initial $^{143}Nd/^{144}Nd$ ratios the initial $^{87}Sr/^{86}Sr$ ratios have an extremely large range of from 0.7030 to 0.7065. This large variation is consistent with hydrothermal interaction of seawater with oceanic crust. In addition, the $^{87}Sr/^{86}Sr$ ratios generally decrease downward (Figure 11), suggesting downward decreasing water/rock ratios. These results indicate that extreme caution must be employed before variations in initial $^{87}Sr/^{86}Sr$ ratios of ophiolitic rocks can be attributed to primary magmatic variations. In this study we have, in fact, found small variations in initial $^{87}Sr/^{86}Sr$ of gabbro plagioclase separates of from 0.70296 ± 2 to 0.70311 ± 5, which we have attributed to primary magmatic variations. However, this interpretation is supported by corresponding variations in the initial $^{143}Nd/^{144}Nd$ ratios and by analysis of coexisting pyroxenes and plagioclases.

5. The complete ^{18}O profile from *Gregory and Taylor* [1981] is also shown in Figure 11. With respect to the "normal" value of $\delta^{18}O = 5.7$ there are both ^{18}O depleted and enriched rocks. The depletions are a result of high-temperature hydrothermal alteration, whereas the ^{18}O enrichments are due to hydrothermal exchange with either strongly ^{18}O-shifted waters at high temperature or less ^{18}O-shifted waters at much lower temperatures.

In Figure 11 there is approximate linear correlation between high ^{18}O and high $^{87}Sr/^{86}Sr$ ratios above the diabase-gabbro contact. Below this contact, the correlation is approximately inverse, corresponding to depleted ^{18}O and high $^{87}Sr/^{86}Sr$ ratios. These relationships are primarily due to the temperature dependence of the oxygen water-rock interactions. Because of this temperature effect it has been shown that, in general, no simple relationship between ^{18}O and $^{87}Sr/^{86}Sr$ variations would be expected for the entire ophiolite section. In fact, at the appropriate temperature of hydrothermal interaction with pristine seawater (200°–250°C) it is possible to

have $^{87}Sr/^{86}Sr$ enrichments while retaining apparently normal ^{18}O values.

Acknowledgments We are particularly indebted to R. G. Coleman and C. A. Hopson who conceived and organized the U.S. Geological Survey/National Science Foundation Oman project. Field work was also conducted with E. H. Bailey and J. S. Pallister. The samples from northern Oman were provided by Bob Coleman who also reviewed the manuscript. This work has benefitted from discussion with M. A. Lanphere, S. B. Jacobsen, R. E. Criss, E. Stolper, and J. Chen. We express our gratitude to the Ministry of Agriculture, Fisheries, Petroleum, and Minerals, Sultanate of Oman, whose hospitality enabled us to conduct field work in Oman. This work has been supported by NSF grants PHY 76-83685, EAR 76-21310, and EAR 78-16874, and indirectly by a grant to C. A. Hopson. Division of Geological and Planetary Sciences, California Institute of Technology, contribution 3303 (317).

REFERENCES

Allegre, C. J., R. Montigny, and Y. Bottinga, Cortege ophiolitique et cortege oceanique, geochimie comparee et mode de genese, *Bull. Soc. Geol. Fr., 15,* 461–477, 1973.

Bailey, E. H. (Compiler), Geologic map of the Muscat-Ibra area, Sultanate of Oman, pocket map, *J. Geophys. Res.,* this issue, 1981.

Boudier, F., and R. G. Coleman, Cross section through the peridotite in the Samail ophiolite, southeastern Oman Mountains, *J. Geophys. Res., 86,* this issue, 1981.

Brooks, C., S. R. Hart, A. Hofmann, and D. E. James, Rb-Sr mantle isochrons from oceanic regions, *Earth Planet. Sci. Lett., 32,* 51–61, 1976.

Carlson, R. W., J. D. Macdougall, and G. W. Lugmair, Differential Sm/Nd evolution in oceanic basalts, *Geophys. Res. Lett., 5,* 229–232, 1978.

Chapman, H. J., and E. T. C. Spooner, ^{87}Sr enrichment of ophiolitic sulphide deposits in Cyprus confirms ore formation by circulating seawater, *Earth Planet. Sci. Lett., 35,* 71–78, 1977.

Chen, J. H., and J. S. Pallister, Lead isotopic studies of the Samail ophiolite, Oman, *J. Geophys. Res., 86,* this issue, 1981.

Christensen, N. I., and M. H. Salisbury, Structure and constitution of the lower oceanic crust, *Rev. Geophys. Space Phys., 13,* 57–86, 1975.

Church, S. E., and M. Tatsumoto, Lead isotope relations in oceanic ridge basalts from the Juan de Fuca-Gorda Ridge area, N.E. Pacific Ocean, *Contrib. Mineral. Petrol., 53,* 253–279, 1975.

Coleman, R. G., Ophiolites ancient oceanic lithosphere?, 229 pp., Springer, New York, 1977.

Corliss, J. B., J. Dymond, L. J. Gordon, J. M. Edmond, R. P. von Herzen, R. D. Ballard, K. Green, D. Williams, A. Bainbridge, K. Crane, and T. H. van Andel, Submarine thermal springs on the Galapagos rift, *Science, 203,* 1073–1083, 1979.

DePaolo, D. J., and G. J. Wasserburg, Nd isotopic variations and petrogenetic models, *Geophys. Res. Lett., 3,* 249–252, 1976*a*.

DePaolo, D. J., and G. J. Wasserburg, Inferences about magma sources and mantle structure from variations of $^{143}Nd/^{144}Nd$, *Geophys. Res. Lett., 3,* 743–746, 1976*b*.

DePaolo, D. J., and G. J. Wasserburg, The sources of island arcs as indicated by Nd and Sr isotopic studies, *Geophys. Res. Lett., 4,* 465–468, 1977.

DePaolo, D. J., and G. J. Wasserburg, Sm-Nd age of the Stillwater complex and the mantle evolution curve for neodymium, *Geochim. Cosmochim. Acta, 43,* 999–1008, 1979.

Duncan, R. A., and W. Compston, Sr-isotopic evidence for an old mantle source region for French Polynesian volcanism, *Geology, 4,* 728–732, 1976.

Edmond, J. M., C. Measures, R. E. McDuff, L. H. Chan, R. Collier, B. Grant, L. I. Gordon, and J. G. Corliss, Ridge crest hydrothermal activity and the balances of the major and minor elements in the ocean: The Galapagos data, *Earth Planet. Sci. Lett., 46,* 1–18, 1979.

Engel, A. E. J., C. G. Engel, and R. G. Havens, Chemical characteristics of oceanic basalts and the upper mantle, *Geol. Soc. Am. Bull., 76,* 719–734, 1965.

Frey, F. A., Rare earth abundances in a high temperature peridotite intrusion, *Geochim. Cosmochim. Acta, 33,* 1429–1447, 1969.

Glennie, K. W., M. G. A. Boeuf, M. W. Hughes-Clarke, M. Moody-Stuart, W. F. H. Pilaar, and B. M. Reinhardt, Geology of the Oman Mountains, *Trans. R. Dutch Geol. Mining Soc. 31,* 423 pp., 1974.

Goldberg, E. D., Minor elements in sea water, in *Chemical Oceanography,* vol. 1, edited by J. P. Riley and G. Skirrow, Academic, New York, 1965.

Green, D. H., W. O. Hibberson, and A. L. Jaques, Petrogenesis of mid-ocean ridge basalts, in *The Earth: Its Origin, Structure and Evolution,* edited by M. W. McElhinny, pp. 265–290, Academic, New York, 1979.

Gregory, R. T., and H. P. Taylor, Jr., An oxygen isotope study of the Cretaceous Samail ophiolite, Oman, Evidence for deep seawater-hydrothermal circulation and implication for spreading center geometry and $\delta^{18}O$ of seawater, *Eos Trans. AGU, 60,* 963, 1979.

Gregory, R. T., and H. P. Taylor, Jr., An oxygen isotope profile in a section of Cretaceous oceanic crust, Samail ophiolite, Oman: Evidence of $\delta^{18}O$-buffering of the oceans by deep (>5 km) seawater-hydrothermal circulation at midocean ridges, *J. Geophys. Res., 86,* this issue, 1981.

Hamilton, P. J., N. M. Evensen, R. K. O'Nions, H. S. Smith, and A. J. Erlank, Sm-Nd dating of Onverwacht Group volcanics, southern Africa, *Nature, 279,* 298–300, 1979.

Hart, R. A., Chemical exchange between seawater and deep ocean basalts, *Earth Planet. Sci. Lett., 9,* 269–279, 1970.

Hawkesworth, C. J., R. K. O'Nions, R. J. Pankhurst, P. J. Hamilton, and N. M. Evensen, A geochemical study of island-arc and back-arc tholeiites from the Scotia Sea, *Earth Planet. Sci. Lett., 36,* 253–262, 1977.

Hedge, C. E., Strontium isotopes in basalts from the Pacific Ocean basin, *Earth Planet. Sci. Lett., 38,* 88–94, 1978.

Hopson, C. A., R. G. Coleman, R. T. Gregory, J. S. Pallister, and E. H. Bailey, Geologic section through the Samail ophiolite and associated rocks along a Muscat-Ibra transect, southeastern Oman Mountains, *J. Geophys. Res., 86,* this issue, 1981.

Irvine, T. N. Crystallization sequences in the Muskox intrusion and other layered intrusions, I, Olivine-pyroxene-plagioclase relations, *Spec. Publ. Geol. Soc. S. Afr., 1,* 444–476, 1970.

Irving, A. J., A review of experimental studies of crystal/liquid trace element partitioning, *Geochim. Cosmochim. Acta, 42,* 743–770, 1978.

Jackson, E. D., The cyclic unit in layered intrusions, *Spec. Publ. Geol. Soc. S. Afr., 1,* 391–424, 1970.

Jackson, E. D., Ultramafic cumulates in the Stillwater, Great Dyke, and Bushveld intrusion, in *Ultramafic and Related Rocks,* edited by P. J. Wyllie, pp. 20–38, John Wiley, New York, 1971.

Jackson, E. D., H. W. Green II, and E. M. Moores, The Vourinos ophiolite, Greece: Cyclic units of lineated cumulates overlying harzburgite tectonite, *Geol. Soc. Am. Bull., 86,* 390–398, 1975.

Jacobsen, S. B., and G. J. Wasserburg, Nd and Sr isotopic study of the Bay of Islands ophiolite complex and the evolution of the source of midocean ridge basalts, *J. Geophys. Res., 84,* 7429–7445, 1979.

Kay, R. W., and R. G. Senechal, The rare earth geochemistry of the Troodos ophiolite complex, *J. Geophys. Res., 81,* 964–970, 1976.

Kay, R. W., N. J. Hubbard, and P. W. Gast, Chemical characteristics and origin of ocean ridge volcanic rocks, *J. Geophys. Res., 75,* 1585–1613, 1970.

Lanphere, M. A., K-Ar ages of metamorphic rocks at the base of the Samail ophiolite, Oman, *J. Geophys. Res., 86,* this issue, 1981.

Lugmair, G. W., K. Marti, J. P. Kurtz, and N. B. Scheinin, History and genesis of lunar troctolite 76535 or: How old is old?, *Proc. Lunar Sci. Conf. 7th,* 2009–2033, 1976.

Malpas, J., Magma generation in the upper mantle, field evidence from ophiolite suites and application to the generation of oceanic lithosphere, *Philos. Trans. R. Soc. London, Ser. A, 288,* 527–546, 1978.

Marsh, B. D., Island-arc volcanism, *Am. Sci., 67,* 161–172, 1979.

Masuda, A., Lanthanide concentrations in the olivine phase of the Brenham pallasite, *Earth Planet. Sci. Lett., 5,* 59–62, 1968.

Mattinson, J. M., Ages of zircons from the Bay of Islands ophiolite complex, western Newfoundland, *Geology, 4,* 393–394, 1976.

McCulloch, M. T., and G. J. Wasserburg, Sm-Nd and Rb-Sr chronology of continental crust formation, *Science, 200,* 1003–1011, 1978.

McCulloch, M. T., R. T. Gregory, G. J. Wasserburg, and H. P. Taylor, Jr., A neodymium, strontium, and oxygen isotopic study of the Cretaceous Samail Ophiolite and implications for the petrogenesis and seawater-hydrothermal alteration of oceanic crust, *Earth Planet. Sci. Lett., 46,* 201–211, 1980.

Montigny, R., H. Bougault, Y. Bottinga, and C. J. Allegre, Trace element geochemistry and genesis of the Pindos ophiolite suite, *Geo-*

chim. Cosmochim. Acta, 37, 2135–2147, 1973.
Moores, E. M., Petrology and structure of the Vourinos ophiolite complex, northern Greece, *Spec. Pap. Geol. Soc. Am., 118,* 1969.
Muehlenbachs, K., and R. N. Clayton, Oxygen isotope studies of fresh and weathered submarine basalts, *Can. J. Earth Sci., 9,* 471–478, 1972.
Muehlenbachs, K., and R. N. Clayton, Oxygen isotope composition of the oceanic crust and its bearing on seawater, *J. Geophys. Res., 81,* 4365–4369, 1976.
Nakamura, N., M. Tatsumoto, P. D. Nunes, D. M. Unruh, A. P. Schwab, and T. R. Wildeman, 4.4 b.y.-old clast in Boulder 7, Apollo 17: A comprehensive chronological study by U-Pb, Rb-Sr, and Sm-Nd methods, *Proc. Lunar Sci. Conf. 7th,* 2309–2333, 1976.
Norton, D., and H. P. Taylor, Jr., Quantitative simulation of the hydrothermal systems of crystallizing magmas on the basis of transport theory and oxygen isotope data: An analysis of the Skaergaard intrusion, *J. Petrol., 20,* 421–486, 1979.
O'Nions, R. K., P. J. Hamilton, and N. M. Evensen, Variations in $^{143}Nd/^{144}Nd$ and $^{87}Sr/^{86}Sr$ ratios in oceanic basalts, *Earth Planet. Sci. Lett., 34,* 13–22, 1977.
O'Nions, R. K., S. R. Carter, R. S. Cohen, N. M. Evens, and P. J. Hamilton, Pb, Nd, and Sr isotopes in oceanic ferromanganese deposits and ocean floor deposits, *Nature, 273,* 435, 1978.
Pallister, J. S., and C. A. Hopson, Samail ophiolite plutonic suite: Field relations, phase variations, cryptic variation and layering, and a model of a spreading ridge magma chamber, *J. Geophys. Res., 86,* this issue, 1981.
Pallister, J. S., and R. J. Knight, Rare-earth element geochemistry of the Samail ophiolite near Ibra, Oman, *J. Geophys. Res., 86,* this issue, 1981.
Peterman, Z. E., C. E. Hedge, and H. Tourtelot, Isotopic composition of Sr in seawater throughout Phanerozoic time, *Geochim. Cosmochim. Acta, 34,* 105–120, 1970.
Peterman, Z. E., R. G. Coleman, and R. A. Hildreth, $^{87}Sr/^{86}Sr$ in mafic rocks of the Troodos massif, Cyprus, *Geol. Surv. Prof. Pap. U.S., 750,* 157D–161D, 1971.
Piepgras, D. J., G. J. Wasserburg, and E. J. Dasch, The isotopic composition of Nd in different ocean masses, *Earth Planet. Sci. Lett., 45,* 223–236, 1979.
Richard, P., N. Shimizu, and C. J. Allegre, $^{143}Nd/^{146}Nd$, a natural tracer: An application to oceanic basalts, *Earth Planet. Sci. Lett., 31,* 269–278, 1976.
Richard, P., D. Rousseau, and C. J. Allegre, Nd and Sr systematics in ophiolites, Short papers of the 4th International Conference on Geochronology, Cosmochronology, and Isotope Geology, *Geol. Surv. Open- File Rep. U.S., 78-701,* 350, 1978.
Schilling, J. G., Sea-floor evolution: Rare-earth evidence, *Philos. Trans. R. Soc. London, Ser. A, 268,* 663–706, 1971.
Schnetzler, C. C., and M. L. Bottino, Some alkali, alkaline earth, and rare earth element concentrations and the Rb-Sr age of the Lost City meteorite and separated phases, *J. Geophys. Res., 76,* 4061–4066, 1971.
Seyfried, W. E., W. C. Shanks, and W. E. Dibble, Clay mineral formation in DSDP leg 34 basalt, *Earth Planet. Sci. Lett., 41,* 265–276, 1978.
Spooner, E. T. C., H. J. Chapman, and J. D. Smewing, Strontium isotopic contamination and oxidation during ocean floor hydrothermal metamorphism of the ophiolitic rocks of the Troodos, Cyprus, *Geochim. Cosmochim. Acta, 41,* 873–890, 1977.
Stern, C., Open and closed system igneous fractionation within two Chilean ophiolites and the tectonic implication, *Contrib. Mineral. Petrol., 68,* 243–258, 1979.
Stolper, E., A phase diagram for mid-ocean ridge basalts: Preliminary results and implications for petrogenesis, *Contrib. Mineral. Petrol.,* in press, 1980.
Suen, C. J., F. A. Frey, and J. Malpas, Bay of Islands ophiolite suite, Newfoundland: Petrologic and geochemical characteristics with emphasis on rare earth element geochemistry, *Earth Planet. Sci. Lett., 45,* 337–348, 1979.
Sun, S. S., and G. N. Hanson, Evolution of the mantle: Geochemical evidence from alkali basalt, *Geology, 3,* 297–302, 1975.
Sun, S. S., M. Tatsumoto, and J. G. Schilling, Mantle plume mixing along the Reykjanes Ridge axis: Lead isotopic evidence, *Science, 190,* 143–147, 1975.
Tatsumoto, M., C. E. Hedge, and A. E. J. Engel, Potassium, rubidium, strontium, thorium, uranium, and the ratio of Sr-87 to Sr-86 in oceanic tholeiitic basalt, *Science, 150,* 886–888, 1965.
Taylor, H. P., Jr., The oxygen isotope geochemistry of igneous rocks, *Contrib. Mineral. Petrol., 19,* 1–71, 1968.
Taylor, H. P., Jr., The application of oxygen and hydrogen isotope studies to problems of hydrothermal alteration and ore deposition, *Econ. Geol., 69,* 843–883, 1974.
Taylor, H. P., Jr., Water/rock interactions and the origin of H_2O in granitic batholiths, *J. Geol. Soc. London, 133,* 509–558, 1977.
Taylor, H. P., Jr., and S. Epstein, Relationship between $^{18}O/^{16}O$ ratios in coexisting minerals of igneous and metamorphic rocks, 1, Principles and experimental results, *Geol. Soc. Am. Bull., 73,* 461–480, 1962.
Taylor, H. P., Jr., and R. W. Forester, An oxygen and hydrogen isotope study of the Skaergaard intrusion and its country rocks: A description of a 55-m.y. old fossil hydrothermal system, *J. Petrol., 20,* 355–419, 1979.
Tilton, G. R., C. A. Hopson, and J. E. Wright, Uranium-lead isotopic ages of the Samail ophiolite, Oman, with applications to Tethyan ocean ridge tectonics, *J. Geophys. Res., 86,* this issue, 1981.
Veizer, J., and W. Compston, $^{87}Sr/^{86}Sr$ composition of seawater during the Phanerozoic, *Geochim. Cosmochim. Acta, 38,* 1461–1484, 1974.
Whitford, D. J., W. Compston, I. A. Nicholls, and M. J. Abbott, Geochemistry of late Cenozoic lavas from eastern Indonesia, role of subducted sediments in petrogenesis, *Geology, 5,* 571–575, 1977.

(Received August 9, 1979;
accepted December 6, 1979.)